

19. X-RAY MINERALOGY STUDIES – LEG 12

Pow-foong Fan¹ and I. Zemmels University of California, Riverside, California²

INTRODUCTION

Semiquantitative determinations of mineral composition in bulk samples from Leg 12 have been performed according to the methods described in the reports of Legs 1 and 2 and in Appendix III of Volume IV. The mineral analyses of the 2-20 μm and $< 2 \mu\text{m}$ fractions from Sites 116 and 117 were performed on calcium carbonate-free residues. The results are presented in Tables 1 to 9 and also in Figures 1 to 21. The ages of the sediments and lithologic units presented in Figures 1 to 21 and used throughout the text of this report are from the data of the DSDP Hole Summaries of Leg 12.

Bentonite gel drilling mud was used in Holes 116 and 117A; mud with barite was used in Holes 112 and 113. There is no detectable contamination of the samples submitted for X-ray mineralogic analysis.

Montmorillonites with two types of expansion behavior were encountered in the samples from Leg 12 similar to those found in Leg 11 samples. The normal expansion to 18Å with trihexylamine acetate was observed in most cases. In some samples, however, montmorillonite which expanded to only 14Å was found. The nonexpanding montmorillonite occurred in pure form as well as in mixtures with normally-expanding montmorillonite. No errors were found in the laboratory procedures and the nonexpanding montmorillonites could be made to expand normally after a brief autoclave treatment. It was found that the height of the peak at 14Å in the nonexpanded form nearly equaled the height of the peak at 18Å in the fully-expanded form after autoclaving. Therefore, the semi-quantitative estimate of montmorillonite based on non-expanded forms is considered to be reasonably accurate.

The type of montmorillonite used in the estimate of montmorillonite in Tables 1 to 9 is designated as follows:

A percentage with no other designation means that the estimate was made from a sample of normally-expanding montmorillonite.

A superscripted (1) is used to indicate that the estimate was made from a 14Å form of montmorillonite. A correction for the 14Å chlorite peak was applied wherever necessary.

A superscript (2) indicates that the determination was made on the sum of both 14Å and 18Å peaks.

RESULTS

Site 111

Site 111 is located on Orphan Knoll, an isolated knoll in the Labrador Sea, 560 kilometers northeast of

¹On leave from Hawaii Institute of Geophysics, University of Hawaii, Honolulu, Hawaii.

²Contribution #464, Hawaii Institute of Geophysics, University of Hawaii. Contribution #72-6. University of California at Riverside, Institute of Geophysics of Planetary Physics.

Newfoundland. A thick sequence of laminated sediments was seen to cap the knoll in seismic reflection profiles. The knoll is thought to be a foundered fragment of the North American continent which broke away in the early stages of sea-floor spreading.

Four lithological units were recognized by shipboard scientists: 1) glacial clays of Pleistocene age interspersed with foraminiferal sandy layers; 2) a Lower Eocene sequence of marls which grade upward into zeolitic clays; 3) dolomite calcarenites, carbonate sands and shelly limestones of Cenomanian age; and 4) a Paleozoic (?) basal unit of coarse graded sandstones and shales. Only the top three units were sampled for X-ray analysis.

Samples of the glacial clays were X-ray analyzed from Cores 1 and 2 in Hole 111 and Cores 1 to 6 in Hole 111A (Figures 1 and 2). Quartz, mica, and plagioclase are the dominant minerals of the glacial clays. Dolomite, montmorillonite, kaolinite and chlorite occur in minor amounts and are present throughout the unit. Amphibole and K-feldspar occur in scattered samples. Dolomite, chlorite and amphibole occur only in the glacial clay unit at Site 111.

A bed of dark, glauconitic silty, foraminiferal sand occurs in Section 3 of Core 6, Hole 111A. This bed was presumed by shipboard scientists to mark the onset of glaciation. It contains lesser amounts of quartz and plagioclase but contains relatively large amounts of calcite, montmorillonite, kaolinite and clinoptilolite (Figure 2). Dolomite, K-feldspar, chlorite, and amphibole were not detected.

Samples from the gradational, Eocene marl-zeolitic clay unit (Cores 7 to 10, Hole 111A) show a decrease in the calcite content upward in the unit (Figure 2). Correspondingly, there is an increase in the quartz and mica contents. Traces of clinoptilolite, kaolinite, plagioclase and relatively large quantities of montmorillonite were detected in the upper, clayey samples.

Samples of Maestrichtian, brownish chalk (Core 11, Hole 111A) consist largely of calcite with traces of K-feldspar (Figure 2). A sample of glauconite sand from the Cenomanian sequence of shallow-water carbonates contains large amounts of quartz, mica and some plagioclase in addition to calcite (Figure 1).

Site 112

Two holes were drilled at Site 112 which was located in the middle of the Labrador Sea. Samples from four lithological units were submitted for X-ray mineralogy analysis.

Pliocene-Pleistocene clays and silts from Cores 1 and 2, Hole 112 and Cores 1 and 3, Hole 112A, consist of quartz, calcite, plagioclase, mica, dolomite, chlorite and amphibole (Figures 3 and 4) much as the Pliocene-Pleistocene

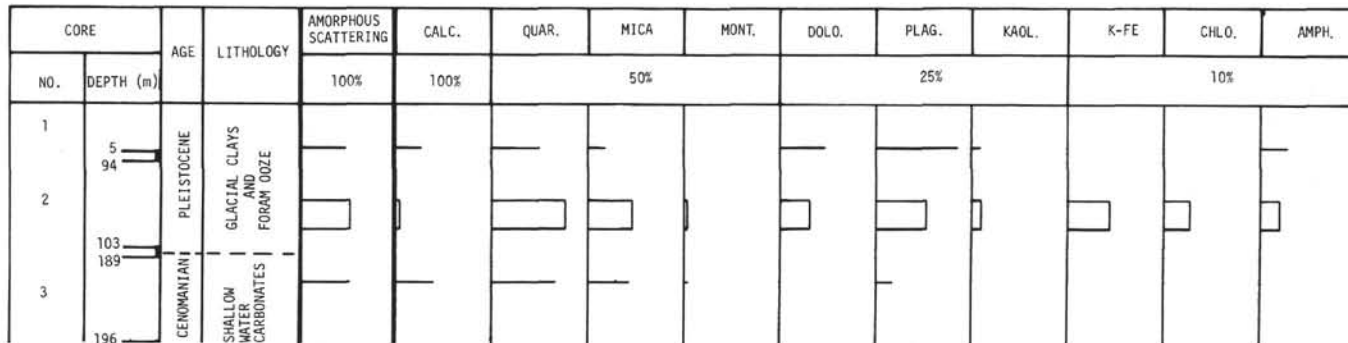


Figure 1. Hole 111. Bulk samples.

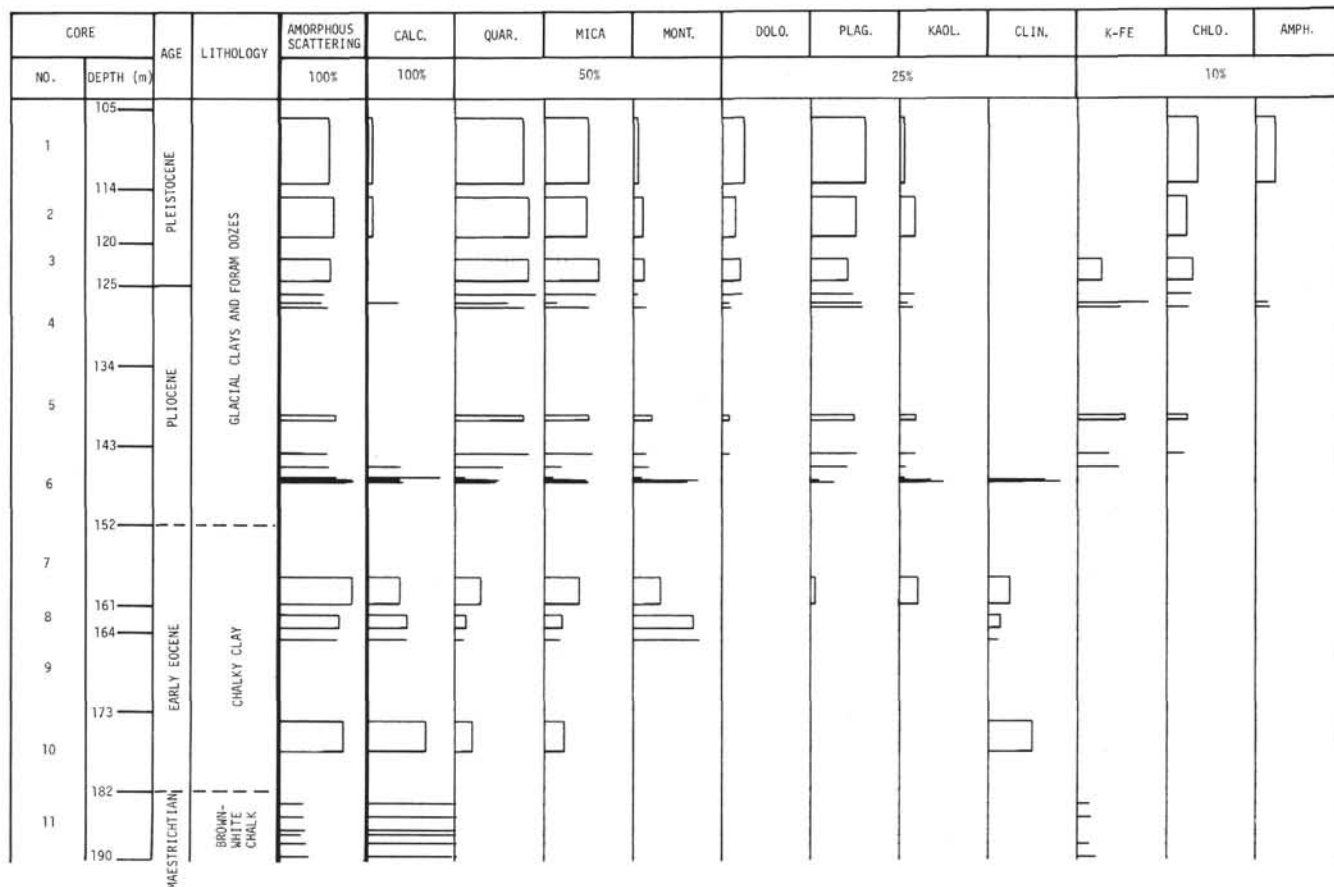


Figure 2. Hole 111A. Bulk samples.

sediments at Site 111. Dolomite and amphibole are restricted to this upper unit as at Site 111. Montmorillonite was not detected in the uppermost samples of the Pliocene-Pleistocene units. A similar paucity of montmorillonite was noted in the Pliocene-Pleistocene hemipelagic muds from the Western Atlantic sampled by Leg 11 (Zemmels *et al* 1972).

The second lithological unit (found in Cores 3 to 11, Hole 112) consists of variably-bedded, gray and brown clay marls and silts with a high content of nannoplankton, diatoms and radiolarians. The age ranges from Oligocene to Miocene. The mineralogy of these units is remarkably uniform despite the variability of the bedding and the variety of sediment types (Core 11 consists of a siliceous ooze). The unit largely consists of calcite, quartz,

montmorillonite, mica and plagioclase (Figure 3). With depth, the ratio of montmorillonite to mica gradually increases (Table 2). Small quantities of kaolinite are found only in the upper portions of this unit. Chlorite occurs sporadically in the upper two lithologic units and is restricted to these units.

An indurated, silty, pelagic, coccolith marl of Lower Oligocene and Upper Eocene age was sampled in Cores 12 to 14. The mineral assemblage of this unit is uniform throughout. Calcite, quartz, montmorillonite and mica are the only minerals detected in the bulk sediments (Figure 2). The montmorillonite content invariably exceeds the mica content in this marl unit by contrast with the overlying mud units where mica usually exceeds montmorillonite.

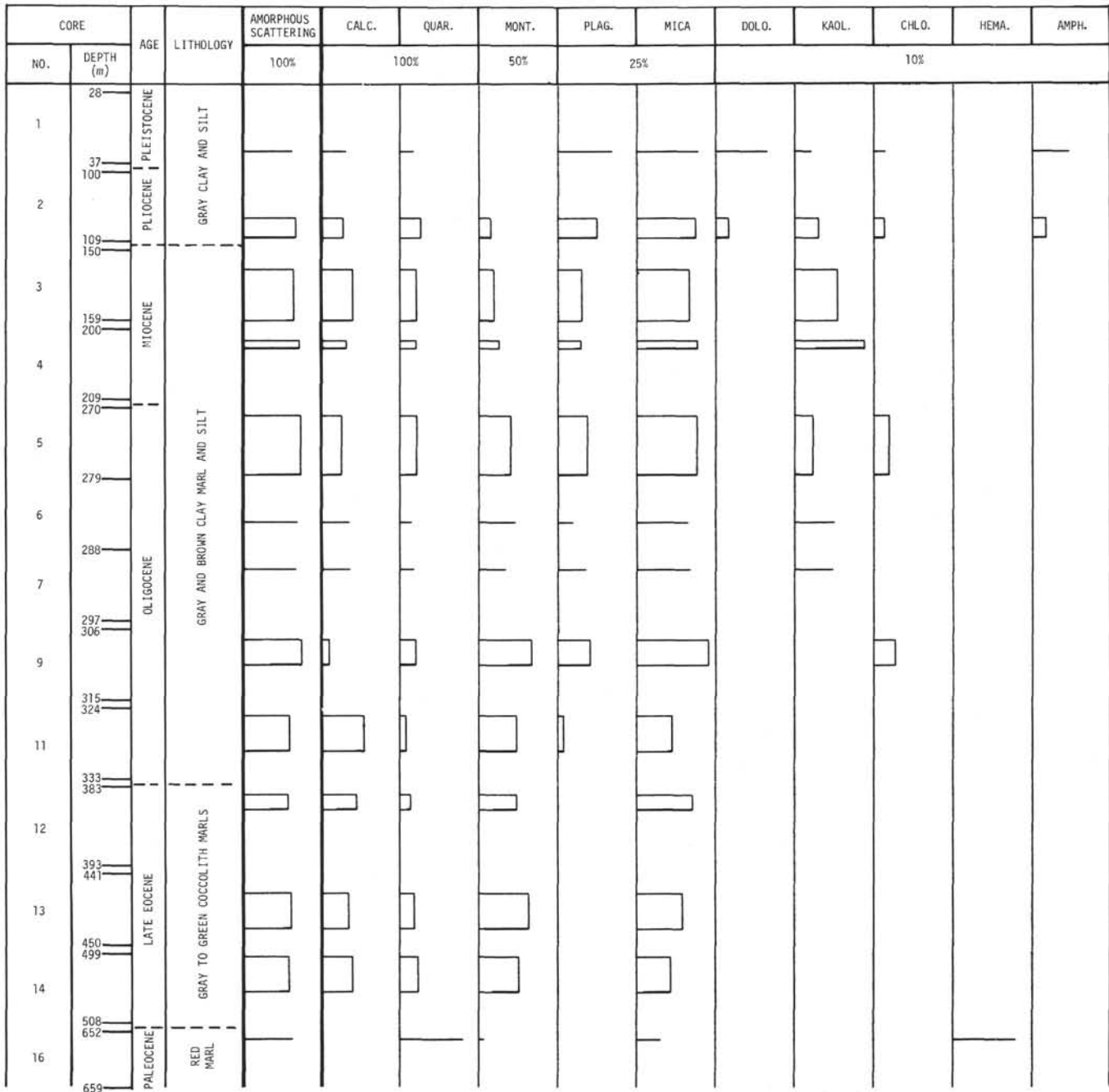


Figure 3. Hole 112. Bulk samples.

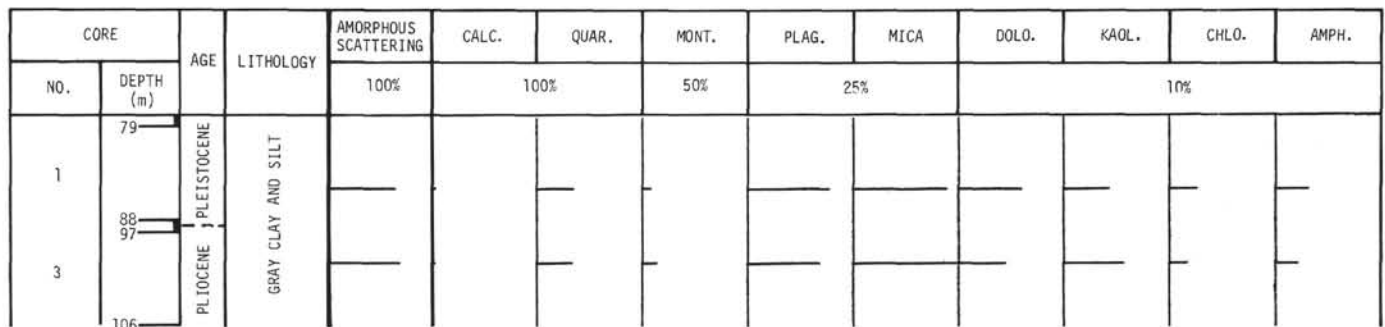


Figure 4. Hole 112A. Bulk samples.

The fourth lithologic unit (found in Core 16, Hole 112, Figure 3) consists of a hard, Paleocene, red, marl clay. The mineral assemblage consists of quartz, mica, hematite and a trace of montmorillonite. There is only two per cent calcite present. Hematite undoubtedly lends the sediment its red color.

Site 113

Site 113 is located just south of the sediment-buried Labrador Sea Ridge. Two lithological units and a turbidite sequence were recognized.

The upper unit (Cores 1 to 4) consists of highly silty glacial muds which contain abundant rock fragments. The predominant minerals in the bulk samples (Figure 5) are quartz, plagioclase and mica. Small amounts of calcite, augite, kaolinite, chlorite and amphibole are found in all the samples of the unit. Montmorillonite is generally found in low concentrations in the Pleistocene unit and was not detected in the uppermost samples of the unit. Dolomite is found only in the upper parts of the unit and, as at Sites 111 and 112, is restricted to the Pleistocene glacial mud units. The augite found in the upper unit may have been derived from submarine basalts in the vicinity of Site 113. However, the general paucity of volcanic glass in the glacial muds, noted by shipboard scientists, makes this source of the augite somewhat questionable.

Pliocene turbidites were recovered from Cores 5 to 7. The sediments consist of sands, alternating layers of clay, a conglomerate of Eocene, Oligocene and Miocene clasts, and contain fossil shallow-water indicators. Mineralogically the turbidite sediments are similar to the overlying Pleistocene muds and the muds of the Eastern North American continental margin, in general, inasmuch as they have high contents of quartz, mica and plagioclase and contain some amphibole, chlorite, and kaolinite. They differ from the overlying sediments in that the turbidites contain clinoptilolite, have a higher montmorillonite content and lack augite and dolomite. Mineralogically, the turbidites resemble the underlying unit far more.

A sequence of Miocene-Pliocene, brown, thinly-laminated, silty mudstones was obtained from Cores 8 to 11. Quartz, mica and plagioclase are the predominant minerals of the bulk sample. The clay minerals kaolinite, chlorite, montmorillonite and mica occur in larger concentrations in the mudstone unit than in the younger glacial muds. The concentrations of quartz and plagioclase are correspondingly diminished (Figure 5). Clinoptilolite and amphibole persist throughout the unit; there is a paucity of calcite. The montmorillonite/mica ratio is considerably higher in the mudstone unit than in the glacial mud unit (Table 3).

Site 114

Site 114 was drilled on the eastern flank of the Reykjanes Ridge in a water depth of 1937 meters and reached basalt 623 meters below the mudline. Lithologically the recovered sediment is essentially structureless and uniform throughout; consists of greenish-gray silty clays and some sandy layers, Pleistocene to Late Miocene in age. From the morphology of some of the seismic reflecting

horizons, shipboard scientists postulated that the sediments were deposited by bottom-contour currents.

A notable change in the mineralogy can be recognized in the bulk sediments at the Pliocene-Pleistocene boundary (Figure 6). The Pleistocene sediments are characterized by the presence of mica, chlorite and montmorillonite, an absence of kaolinite and pyrite and a slightly larger quartz-content than the older sediments. Calcite, plagioclase, and augite are abundant throughout the section. Clay minerals are largely not detected in the bulk sediments by contrast with sediments deposited from bottom-contour currents along the eastern continental margin of North America (Zemmels *et al.*, 1972). This implies that the contour currents along the North American continental margin have a rather different origin than the contour current along the Reykjanes Ridge, probably originating from the Norwegian Sea (Johnson and Schneider, 1969). The entire section is highly X-ray amorphous (Figure 6 and Table 4) due to the presence of diatoms, sponge spicules and volcanic glass. The absence of detectable quantities of clay minerals may be accounted for, in part, by the effect of dilution by the amorphous material.

The most abundant detrital minerals, plagioclase and augite are probably derived from submarine basalt in the vicinity of Site 114. The low content of quartz and mica give the sediments a pelagic aspect. Pyrite is found commonly in the Miocene-Pliocene sediments and occurs as fillings and replacements of siliceous tests (Figure 6).

Site 115

Site 115 was located in a basin between the Reykjanes Ridge and the Rockall Plateau. Eight cores were recovered from this site all of which consisted of hard, graded volcanic sandstones consisting or reworked pyroclastic detritus. The volcanic sandstone deposit is very extensive and seems to be derived from submarine basalt in the vicinity of Site 115. Only one sample of Pleistocene dark gray, laminated tuff from Core 4 was submitted for X-ray mineralogic analysis. The sample has a large amorphous content (Table 5). The crystalline phase primarily consists of plagioclase and augite. Small amounts of quartz and kaolinite were detected which may be from admixed pelagic materials (Figure 7 and Table 5). Small quantities of analcite are also present.

Sites 116 and 117

The Hatton-Rockall Basin, between Hatton and Rockall Banks, is part of the Rockall Plateau—a large, well-defined shoal area located between Iceland and Ireland. The Rockall Plateau is believed to be a continental fragment which was separated from Europe and Greenland during the opening of the North Atlantic Ocean. Site 116 was drilled in the center of the basin where a thick sequence of sediments was found. Site 117 was drilled on the eastern rim of the basin (on Rockall Bank) at a location where some of the deepest seismic reflecting horizons seen at Site 116 had been traced to the surface. Four holes were drilled (116, 116A, 117 and 117A) and a nearly-complete sequence from Pleistocene to Paleocene was recovered with little overlapping of sections. Hole 117A encountered basalt.

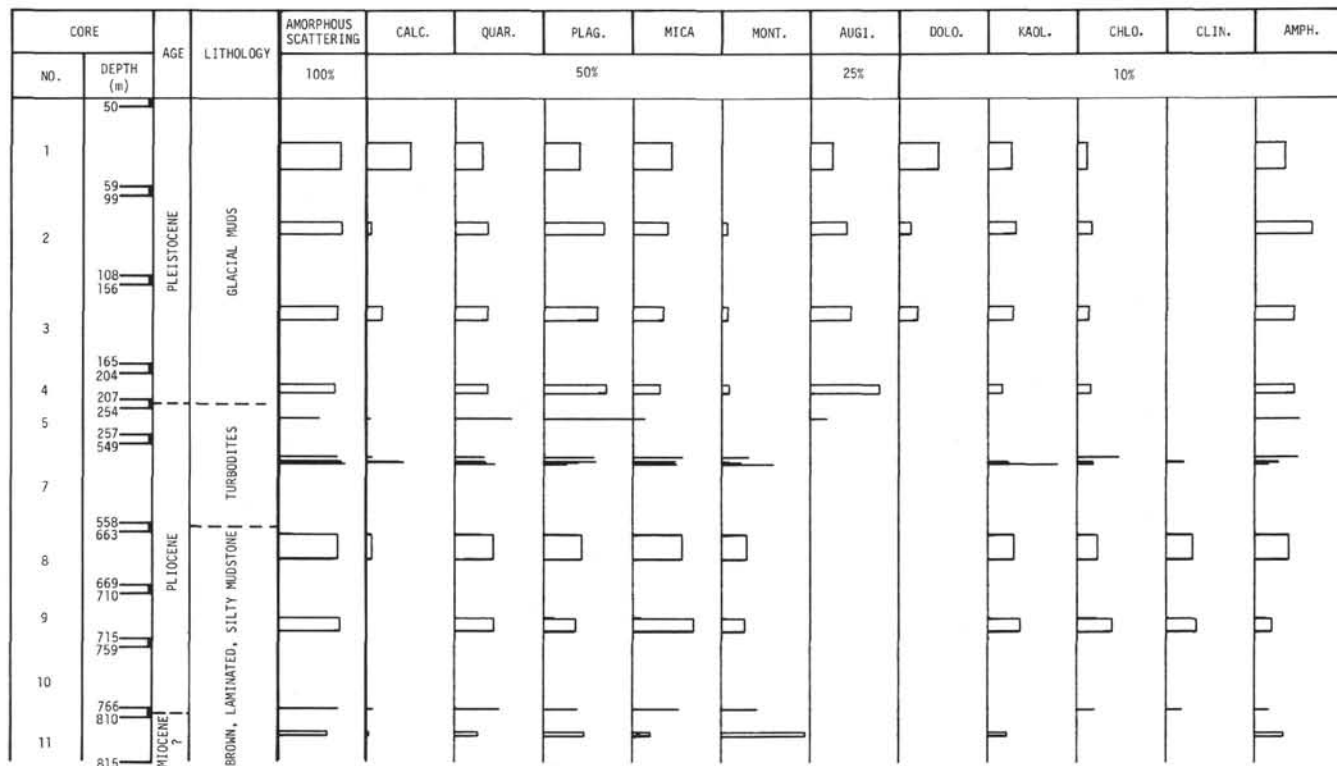


Figure 5. Hole 113. Bulk samples.

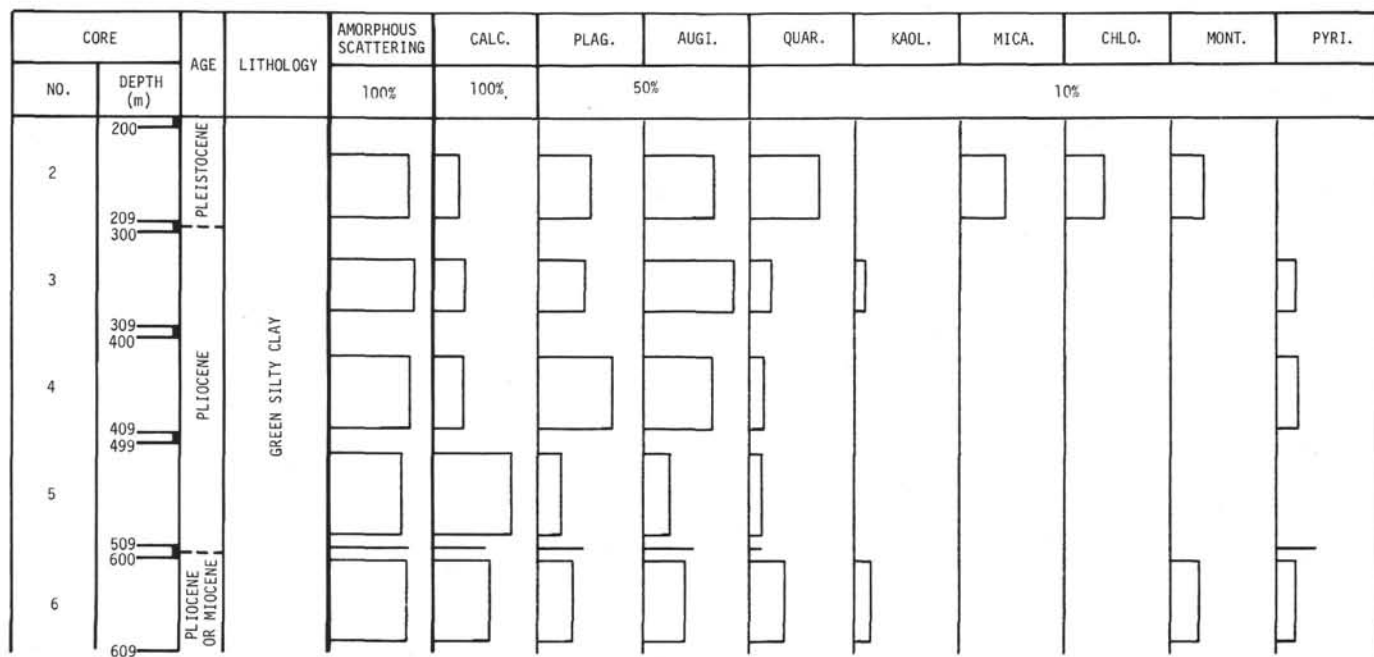


Figure 6. Hole 114. Bulk samples.

The upper lithologic unit consists of a foraminiferal-nannofossil ooze with silt and clay, Pleistocene to Late Pliocene in age. The unit is found in Cores 1 to 8 in Hole 116A. The calcite content is generally high in the bulk samples (Figure 11). Quartz, plagioclase and mica are the predominant minerals of the detrital phase in the sediment—an assemblage which is characteristic of

continentally derived detritus. The clay minerals kaolinite, chlorite and montmorillonite were detected only in a few scattered samples.

Quartz, mica and plagioclase are the major minerals of the decalcified 2 to 20-micrometer fraction. K-feldspar and chlorite persist throughout the unit. Augite and kaolinite were found in a number of samples. Amphibole

CORE		AGE	LITHOLOGY	AMORPHOUS SCATTERING	PLAG.	AUGI.	QUAR.	KAOL.
NO.	DEPTH (m)			100%	50%		10%	
4	100 107	PLEISTOCENE	TUFF	—	—	—	—	—

Figure 7. Hole 115. Bulk samples.

is found to be restricted to the six uppermost cores (Figure 12).

The $<2 \mu\text{m}$ fraction contains large concentration of quartz and mica. Montmorillonite, kaolinite chlorite and plagioclase persist throughout the unit. The mica concentration exceeds the montmorillonite concentration throughout (Table 6).

The muddy Pliocene-Pleistocene sediments are underlain by a thick sequence of highly calcareous sediments which can be divided into several lithologic units. A light gray and greenish, foraminiferal-nannofossil ooze, found in Cores 1 to 6 in Hole 116 and Cores 9 to 11 in Hole 116A and a bluish-white, foraminiferal-nannofossil ooze, found in Cores 7 to 17 in Hole 116, are not readily distinguishable mineralogically and will be discussed together here.

The oozes are Late Pliocene to Early Miocene in age. Only calcite was detected in all but a few bulk samples (Figures 8, 11). The decalcified 2-20 μm fractions contain large quantities of quartz, plagioclase and mica as in the overlying unit (Figures 9, 12). Pyrite is prevalent throughout the section. Clinoptilolite, phillipsite barite and augite were detected in a few scattered samples. A sample from Core 9, Hole 116 consisted entirely of celestite.

The decalcified $<2 \mu\text{m}$ fraction of the foraminiferal-nannofossil ooze unit contains large quantities of quartz and mica (Figures 10, 13). Montmorillonite occurs throughout the formation and becomes increasingly abundant with depth. Kaolinite is restricted to the upper portions of the unit. Plagioclase and K-feldspar were frequently detected. Cristobalite, apatite, clinoptilolite, pyrite and gypsum were detected in a few scattered samples.

The presence of halite in a number of samples in the lower part of the unit is noteworthy. Considering the large volume of liquid that the $<2 \mu\text{m}$ fraction passes through in the decalcification and size-centrifuging procedures, it is evident that the halite which is found here must have been completely occluded or extensively armored to avoid dissolution. An understanding of the mechanism of halite occlusion would be of considerable interest to students of the geochemistry of sodium and chlorine.

A thin-bedded, chalk and foraminiferal-nannofossil ooze unit of Early Miocene to Early Oligocene age was recovered in Cores 20 to 23 in Hole 116 (Figures 8, 9 and 10). Core 20, consisting mostly of chalk, contains an unusually large quantity of montmorillonite in the bulk sample (Figure 8) which is also seen in the $<2 \mu\text{m}$ fraction (Figure 10). The remaining samples in this unit are high in calcite with only

traces of cristobalite and clinoptilolite being detected in the bulk (Figure 8). The 2-20 μm fraction is seen to contain large quantities of cristobalite and clinoptilolite, as well as some quartz, plagioclase and mica. Quartz, plagioclase, mica and pyrite persist throughout. The $<2 \mu\text{m}$ fraction is largely made up of cristobalite and is virtually barren of clay minerals with the exception of a few traces of montmorillonite and mica. The montmorillonite content generally exceeds the mica content (Figure 10).

A unit of chalky limestone, Early Oligocene to Late Eocene in age, sampled in Cores 26 and 27, Hole 116, mineralogically resembles the overlying chalk ooze unit in nearly every respect (Figures 8, 9 and 10).

Cherty limestones of Late Eocene age were encountered in Core 2, Hole 117 and Core 1, Hole 117A. All the size fractions show large quantities of cristobalite and clinoptilolite. Detrital minerals such as quartz, plagioclase, and mica are low or absent. Montmorillonite is the predominant clay mineral (Figures 14 to 19).

Basal sediments, in contact with basalt, consisting of a reworked-volcanic-material, sandy conglomerate, silty clays, and mudstones of early Eocene and Late Paleocene age were sampled from Cores 3, 4, and 6 of Hole 117A (Figures 17 to 19). The presence of a phosphorite nodule and fossil shallow-water species suggest a shallow-water origin for these sediments. The mineralogy is rather variable but generally the calcite content is low, montmorillonite is the dominant mineral of the bulk and $<2 \mu\text{m}$ fractions, and clinoptilolite is abundant in all the fractions. Diminutive amounts of the detrital minerals plagioclase, quartz, K-feldspar, and kaolinite are found. Barite, pyrite, anatase and magnetite were also detected. Occluded halite is found in the $<2 \mu\text{m}$ fraction.

Site 118

Hole 118 was drilled on the western margin of the Bay of Biscay abyssal plane near a basement high which rises close to the sediment surface. Two major lithologic units were recognized.

The younger unit consists of a thick sequence of normal pelagic sediments interbedded with turbidites of Pleistocene to Middle Miocene age (Cores 1 to 11). This sequence has been divided into four subunits (as in Figure 20) which differ from one another mineralogically only in minor respects. Calcite, quartz and mica make up the major portion of the bulk fraction. Plagioclase and kaolinite are detected throughout the unit in the low-calcareous

CORE		AGE	LITHOLOGY	AMORPHOUS SCATTERING	CALC	QUAR	CRIS	MICA	MONT	CLIN
NO.	DEPTH (m)			100%	100%	50%	25%		10%	
1	70	LATE PLEISTOCENE	LIGHT GRAY AND GREENISH FORAM-NANNOFOSSIL OOZE							
	79									
2	109	EARLY PLEISTOCENE								
	116									
3	159	LATE MIOCENE								
	166									
4	209	LATE MIOCENE								
	216									
5	259	LATE MIOCENE								
	268									
6	309	LATE MIOCENE								
	316									
7	359	MIDDLE MIOCENE								
	368									
8	409	MIDDLE MIOCENE								
	418									
9	459	MIDDLE MIOCENE								
	468									
10	509	MIDDLE MIOCENE								
	518									
11	559	MIDDLE MIOCENE								
	568									
12	599	MIDDLE MIOCENE								
	608									
15	662	MIDDLE MIOCENE								
	671									
16	680	EARLY MIOCENE								
	689									
17	701	EARLY MIOCENE								
	710									
20	719	EARLY MIOCENE								
	728									
21	750	EARLY MIOCENE								
	759									
22	825	EARLY OLILOCENE								
	831									
23	840	LATE EOCENE								

Figure 8. Hole 116. Bulk samples.

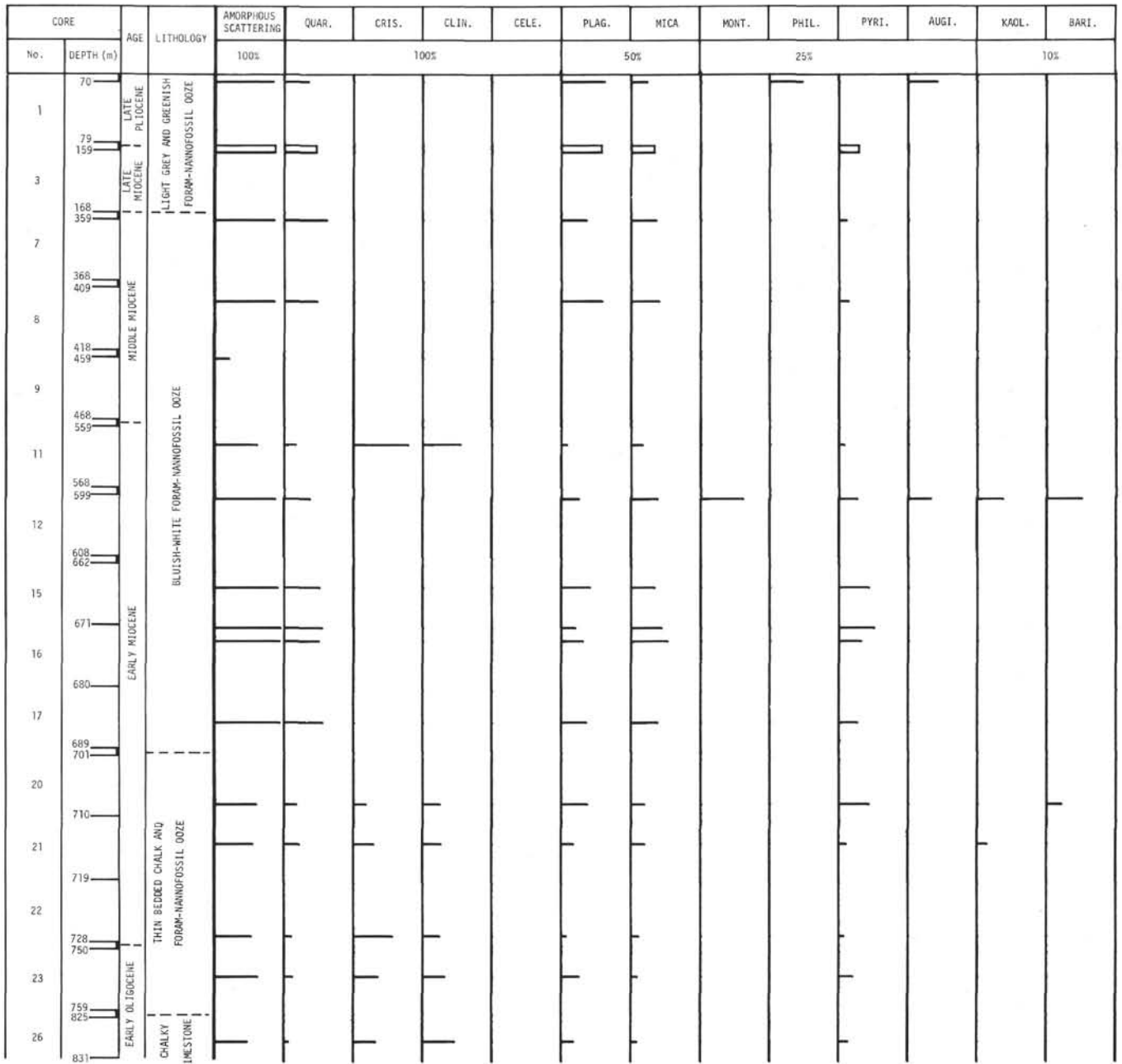


Figure 9. Hole 116. 2-20 μm fractions.

sediments. Chlorite occurs only in the upper parts of the unit. Montmorillonite was not detected in the uppermost Pliocene-Pleistocene sediments, but is rather prominent in deeper samples. Aragonite and dolomite are associated with carbonate sandstones in Cores 6, 7 and 8 (Figure 20).

The second lithologic unit consists of Early Eocene to Paleocene red clay. The unit has been further divided into an upper subunit of slightly altered brown and gray clays with nannofossils (Core 13) and a lower subunit of hard, red and brown altered clays without nannofossils (Cores 15 to 19). The upper unit consists mostly of calcite with minor amounts of quartz, mica, kaolinite and montmorillonite. The lower, altered unit contains no calcite. Quartz and plagioclase are present. Mica and kaolinite are the most prevalent clay minerals. Montmorillonite is of minor

importance and chlorite is absent. Clinoptilolite was detected in Core 16. Hematite was sought but was not detected by X-ray techniques. The amorphous scattering value is comparatively high in the altered clay unit.

Site 119

Hole 119 was drilled on top of Cantabria Seamount which probably is an uplifted portion of the sea floor in the Bay of Biscay. Four lithologic units were recognized (Figure 21).

Cores 1 and 2 consist of Pleistocene olive gray, silty clays. Calcite, quartz and mica make up the major portion of the bulk fraction. Small amounts of kaolinite, chlorite, montmorillonite, dolomite and plagioclase were detected. Chlorite is restricted to the Pleistocene sediments at Site

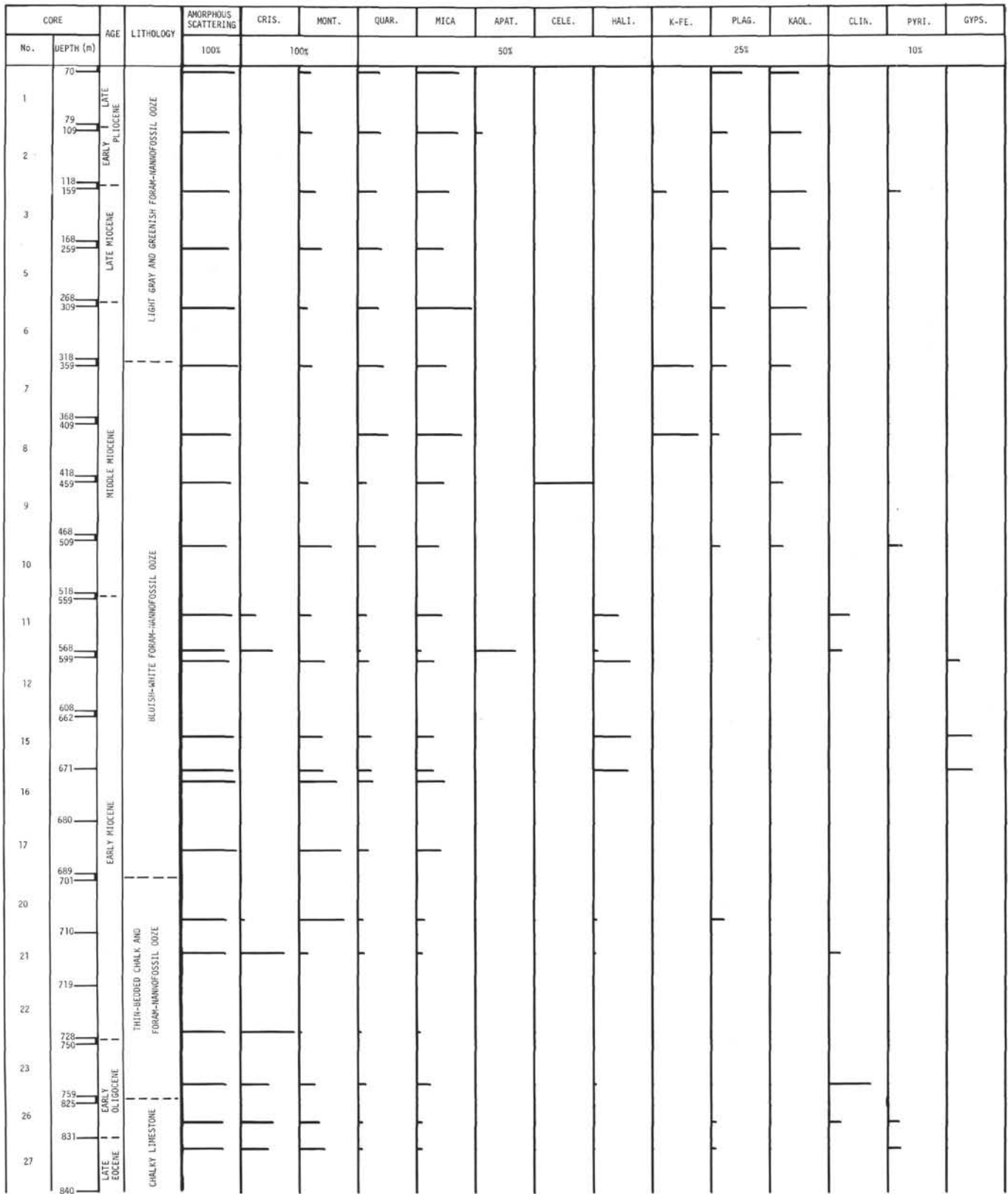


Figure 10. Hole 116. <math>< 2 \mu\text{m}</math> fractions.

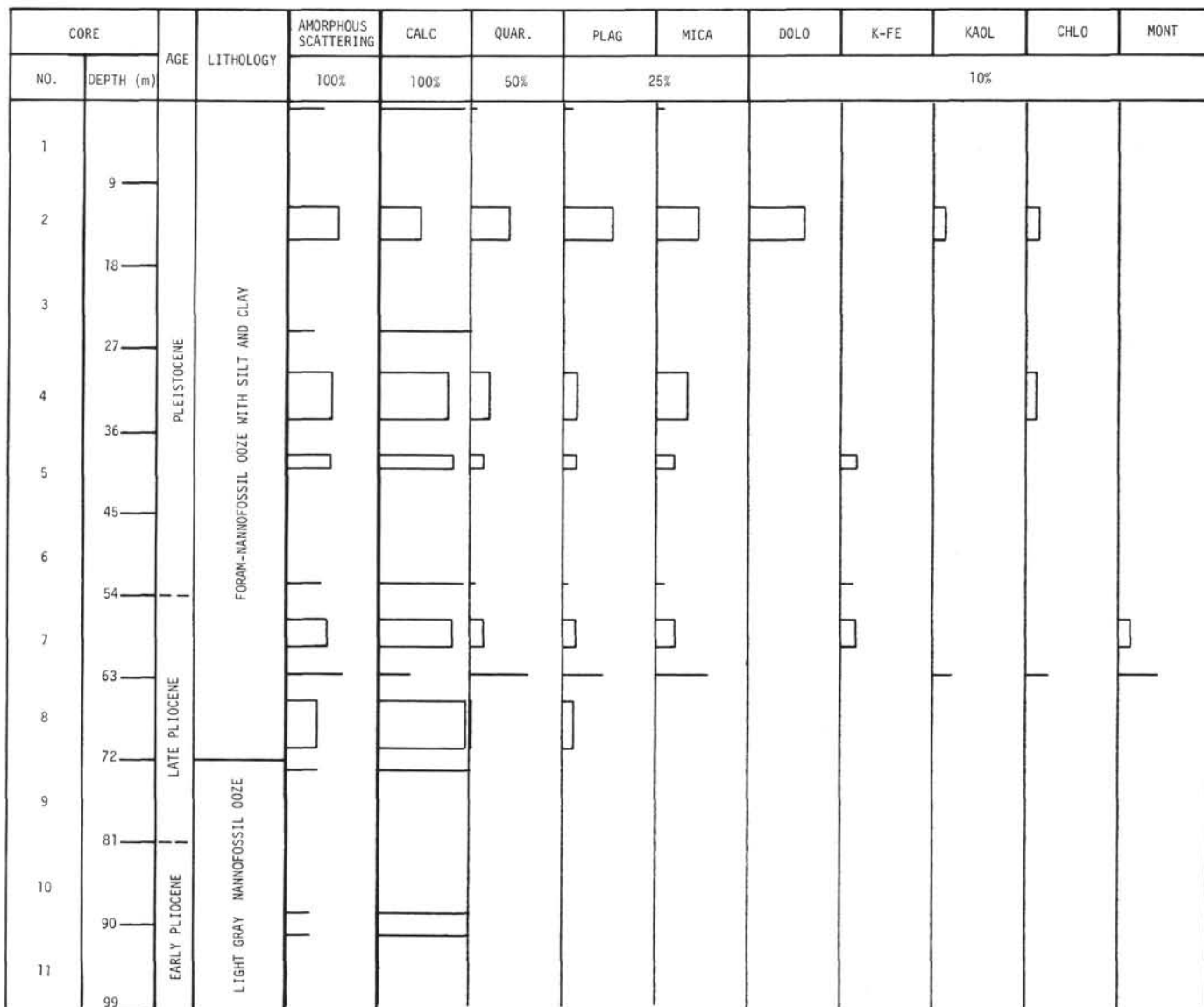


Figure 11. Hole 116A. Bulk samples.

119. Jones and Funnell (1969) have inferred the presence of a dolomite-bearing Cretaceous outcrop on Cantabria Seamount in the vicinity of Site 119 which may be the source of dolomite in the Pleistocene clays.

Massive gray, greenish-gray and yellow nannofossil clays, Pliocene to Oligocene in age, were recovered in Cores 3 to 18. The nannofossil clays become more calcite-rich with depth. Quartz, mica, plagioclase, kaolinite and montmorillonite are abundant at the top of the clay unit and diminish with depth, probably as a result of dilution by calcite. The occurrence of clinoptilolite is restricted to the lower parts of the unit.

The third lithologic unit consists of thin-bedded, Eocene, red, brown, and gray clays (Cores 19 to 22). Mineralogically the unit is indistinguishable from the overlying unit except for the presence of palygorskite (Figure 21).

The fourth lithologic unit is a thick Paleocene sequence of green nannofossil marl extensively interbedded with marl

turbidites (Cores 25 to 40). In addition to calcite, the predominant minerals throughout the unit are mica, quartz, plagioclase and montmorillonite. Kaolinite was not detected in the Paleocene turbidite sequence (except for Core 38). Clinoptilolite is prominent in the upper portions of the unit. Cristobalite and palygorskite were found at a few scattered localities (Figure 21).

DISCUSSION

Clinoptilolite is found at several sites in sediments widely varying in age and type: Eocene chalky clays (111A), Pliocene silty muds (113), Oligocene limestone and calcareous ooze (116), Late Eocene cherty limestone (117), Eocene clays (118) and Oligocene nannofossil-rich clays (119). In general, clinoptilolite is associated with pelagic muds or the muddy facies of calcareous sediments. No strong correlation with pyroclastic materials has been observed in Leg 12 or Leg 11 materials.

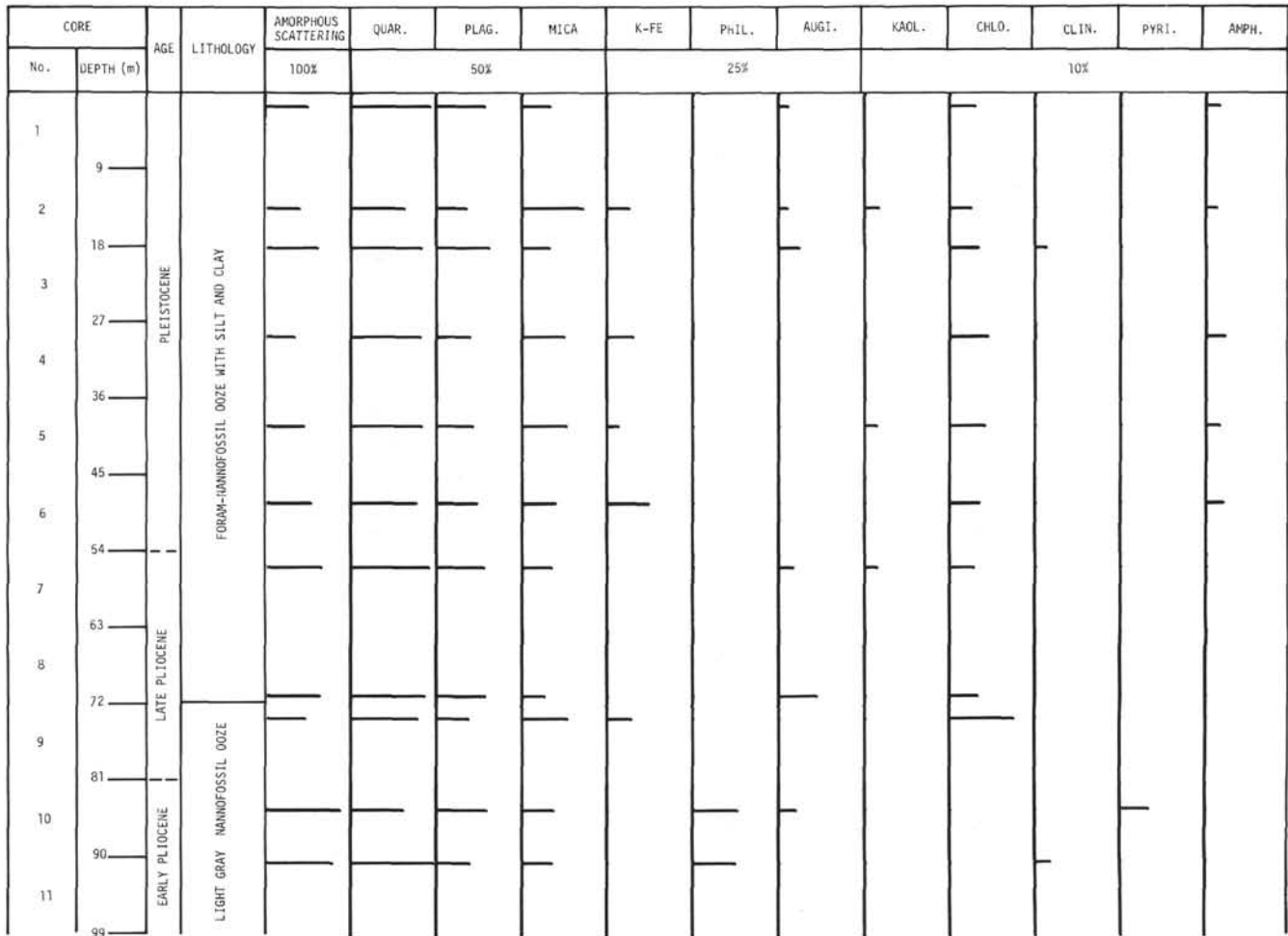


Figure 12. Hole 116A. 2-20 μm fractions.

Palygorskite was found in the bulk sample of Eocene brown, pelagic clays at Site 119.

Celestite was discovered in Core 9, Hole 116 in a massive unit of Miocene foraminiferal-nannofossil ooze. Most of the celestite occurs as very fine-grained aggregates with crystals less than 2 micrometers in diameter. The mean refractive index of the aggregates is 1.62. A few columnar crystals, about 10 microns long, were also seen.

CONCLUSIONS

The Leg 11 coring sites covered a wide area — a traverse across the northern portion of the Atlantic Ocean. Regional correlation is difficult because the sediments which were encountered contained numerous turbidite units and lithologic units deposited by bottom currents. The sedimentary facies in these cases largely reflect local depositional environments.

Mineralogical changes across the Pliocene-Pleistocene boundary can be seen in all of the holes on Leg 11 which contain the boundary. The Pleistocene sediments are typically characterized by a larger clay mineral content than the Pliocene sediments. The high concentration of clay minerals in the Pleistocene deposits is probably due to a

contribution from glacial tills and increased erosion due to the melting of the ice sheets. Jacobs (1970) noted that fine-grained detrital chlorite was released during the continental glaciation to produce a Pleistocene imprint on ocean sediments.

Four sedimentary suites are recognized at the nine coring sites:

(1) The Northwestern Atlantic Suite (Sites 111, 112, and 113) is characterized by sediments which contain large quantities of quartz, mica and plagioclase and small but ever-present amounts of kaolinite and chlorite. The mineral assemblages of these sites are very similar to those reported by Marlowe (1969) in Tertiary strata off Nova Scotia and by Phipp and King (1969) from the Scotian Shelf. Dolomite was found frequently in the Pleistocene deposits in this study but was not mentioned in the published reports from this area. The dolomitic sedimentary rocks of the St. George Formation (Ordovician?) of Newfoundland, which is part of the Appalachian Mountain system (Palmer, 1969) may be the source of the dolomite found at Sites 111, 112 and 113.

(2) The Central Atlantic Suite (Sites 114 and 115) consists of pelagic sediments and locally-derived volcanic sediments. They are characterized by the presence of glass,

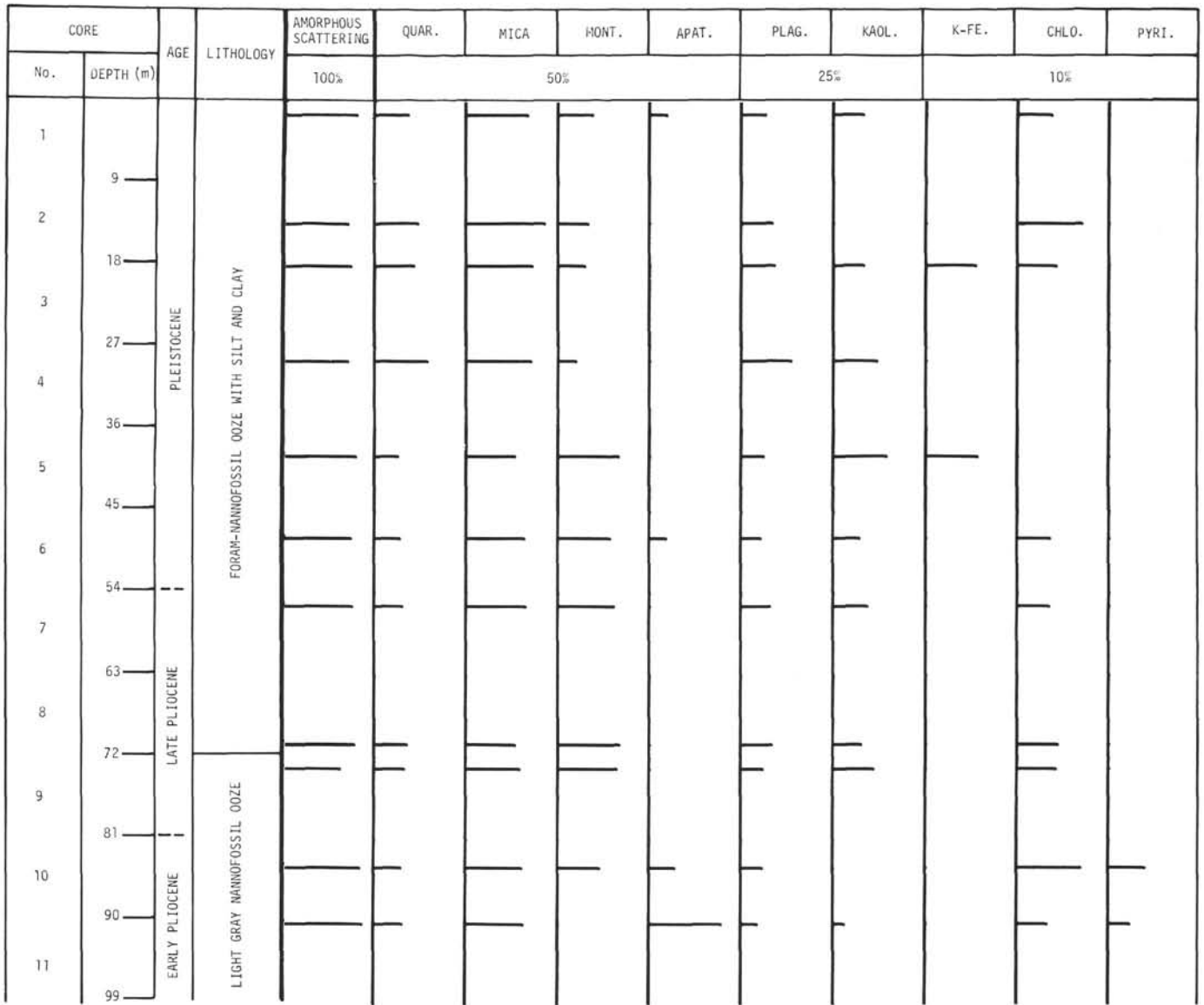


Figure 13. Hole 116A. <math>< 2 \mu\text{m}</math> fractions.

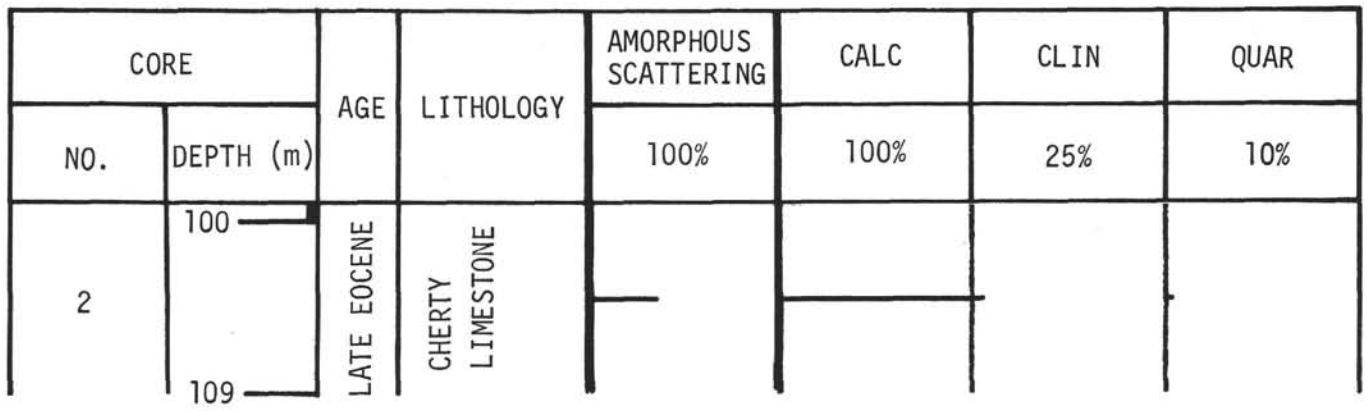


Figure 14. Hole 117. Bulk samples.

CORE		AGE	LITHOLOGY	AMORPHOUS SCATTERING	CLIN.	QUAR.	K-FE.	PLAG.	MICA
No.	DEPTH (m)			100%	100%	10%			
2	100-109	LATE EOCENE	CHERTY LIMESTONE	—	—	—	—	—	—

Figure 15. Hole 117. 2-20 μm fractions.

CORE		AGE	LITHOLOGY	AMORPHOUS SCATTERING	MICA	MONT.	CLIN.	QUAR.
No.	DEPTH (m)			100%	50%		25%	10%
2	100-109	LATE EOCENE	CHERTY LIMESTONE	—	—	—	—	—

Figure 16. Hole 117. <2 μm fractions.

CORE		AGE	LITHOLOGY	AMORPHOUS SCATTERING	CALC.	MONT.	PLAG.	CLIN.	QUAR.	K-FE.	KAOL.	AUGI.
NO.	DEPTH (m)			100%	100%		25%		10%			
1	146	EARLY/LATE EOCENE	CHERTY LIMESTONE	—	—	—	—	—	—	—	—	—
3	155-222			—	—	—	—	—	—	—	—	—
4	227-276	LATE PALEOCENE	OLIVE-GRAY CLAY	—	—	—	—	—	—	—	—	—
6	285			—	—	—	—	—	—	—	—	—

Figure 17. Hole 117A. Bulk samples.

CORE		AGE	LITHOLOGY	AMORPHOUS SCATTERING	CLIN.	CRIS.	K-FE.	BARI.	QUAR.	MONT.	MAGN.	PYRI.
No.	DEPTH (m)			100%	100%	50%		25%	10%			
7	146	LATE EOCENE	CHERTY LIMESTONE	—	—	—	—	—	—	—	—	—
4	155-276			—	—	—	—	—	—	—	—	—
6	285	LATE PALEOCENE	OLIVE-GRAY CLAY	—	—	—	—	—	—	—	—	—

Figure 18. Hole 117A. 2-20 μm fractions.

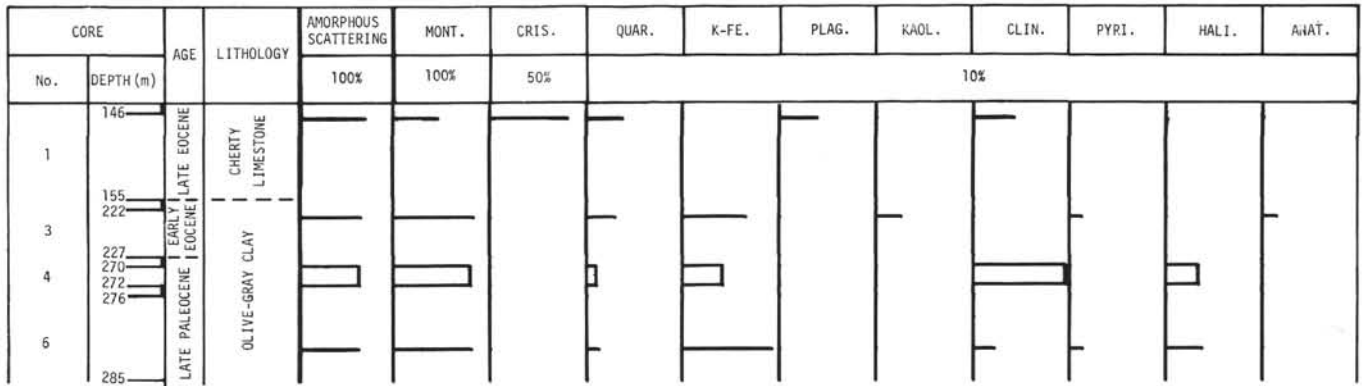


Figure 19. Hole 117A. <math>< 2 \mu\text{m}</math> fractions.

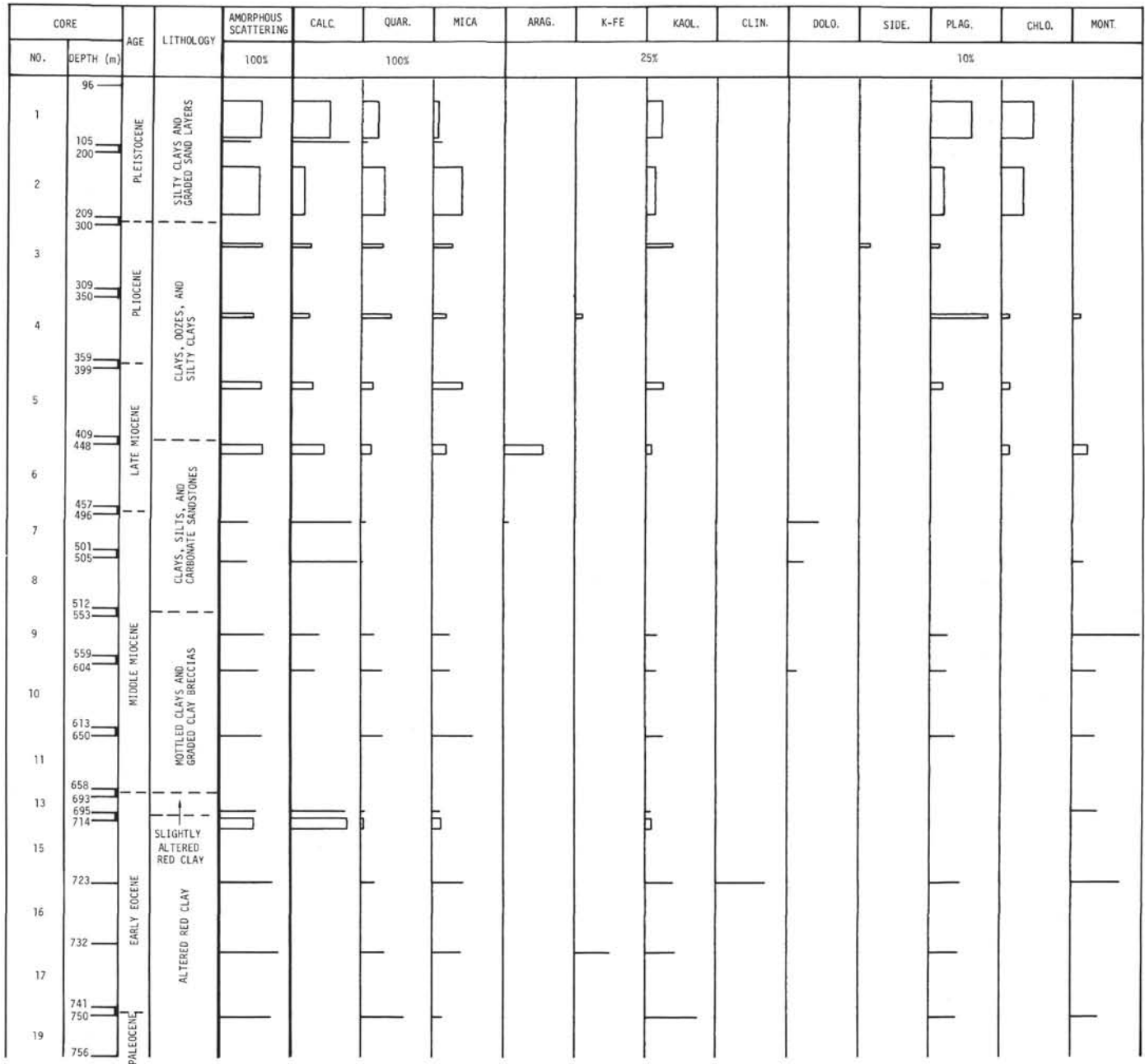


Figure 20. Hole 118. Bulk samples.

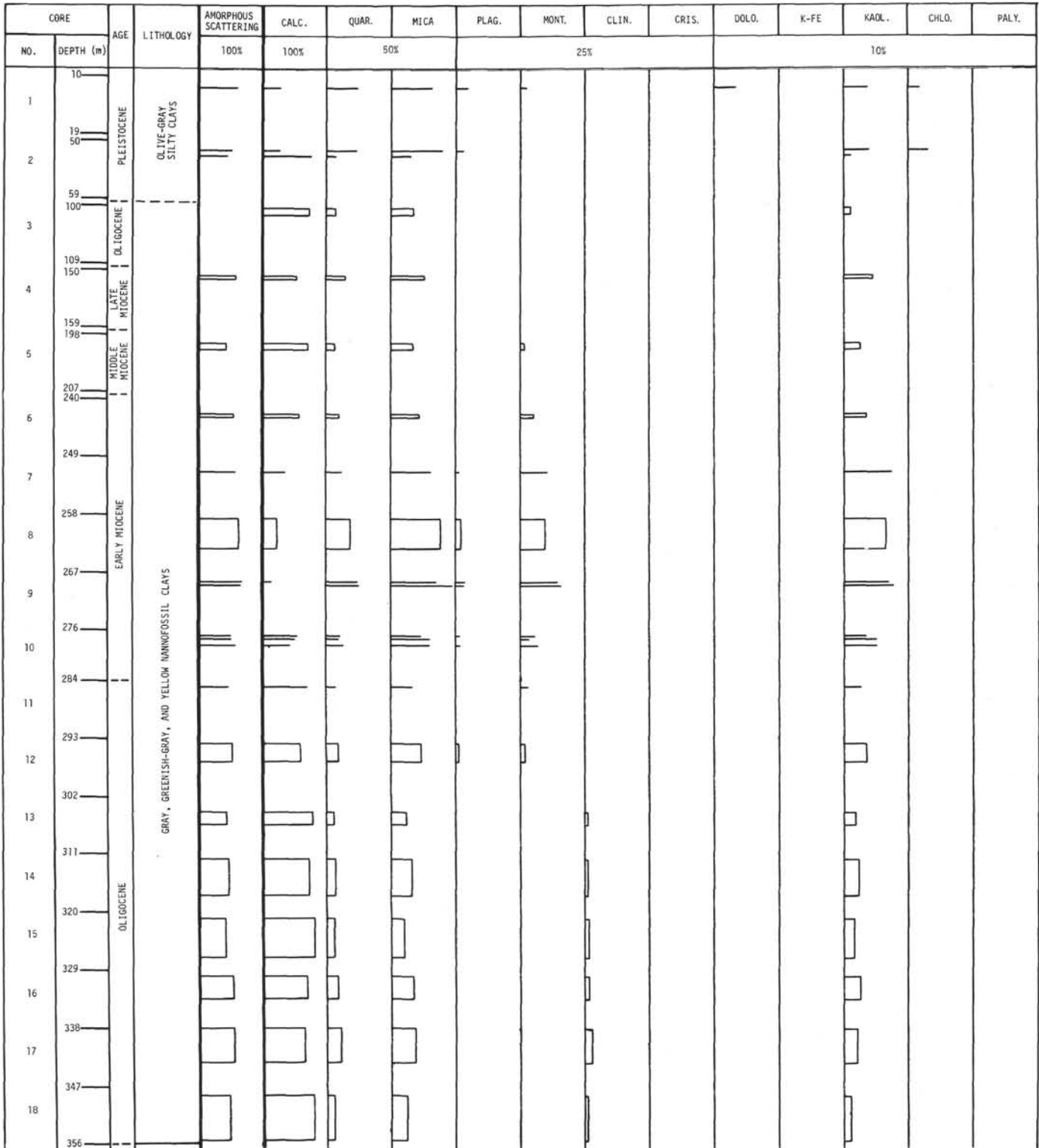


Figure 21. Hole 119. Bulk samples.

amorphous silica, augite and plagioclase. They typically have low quartz and clay minerals contents. The sediments are probably derived in large part from pillow basalts on the Reykjanes Ridge which reflect this composition (Boer *et al.*, 1969).

(3) The Rockall Plateau Suite (Sites 116 and 117) is characterized by sediments which are abundant in quartz and mica with some K-feldspar, suggestive of continental affinities, but with a low clay minerals content and a paucity of chlorite.

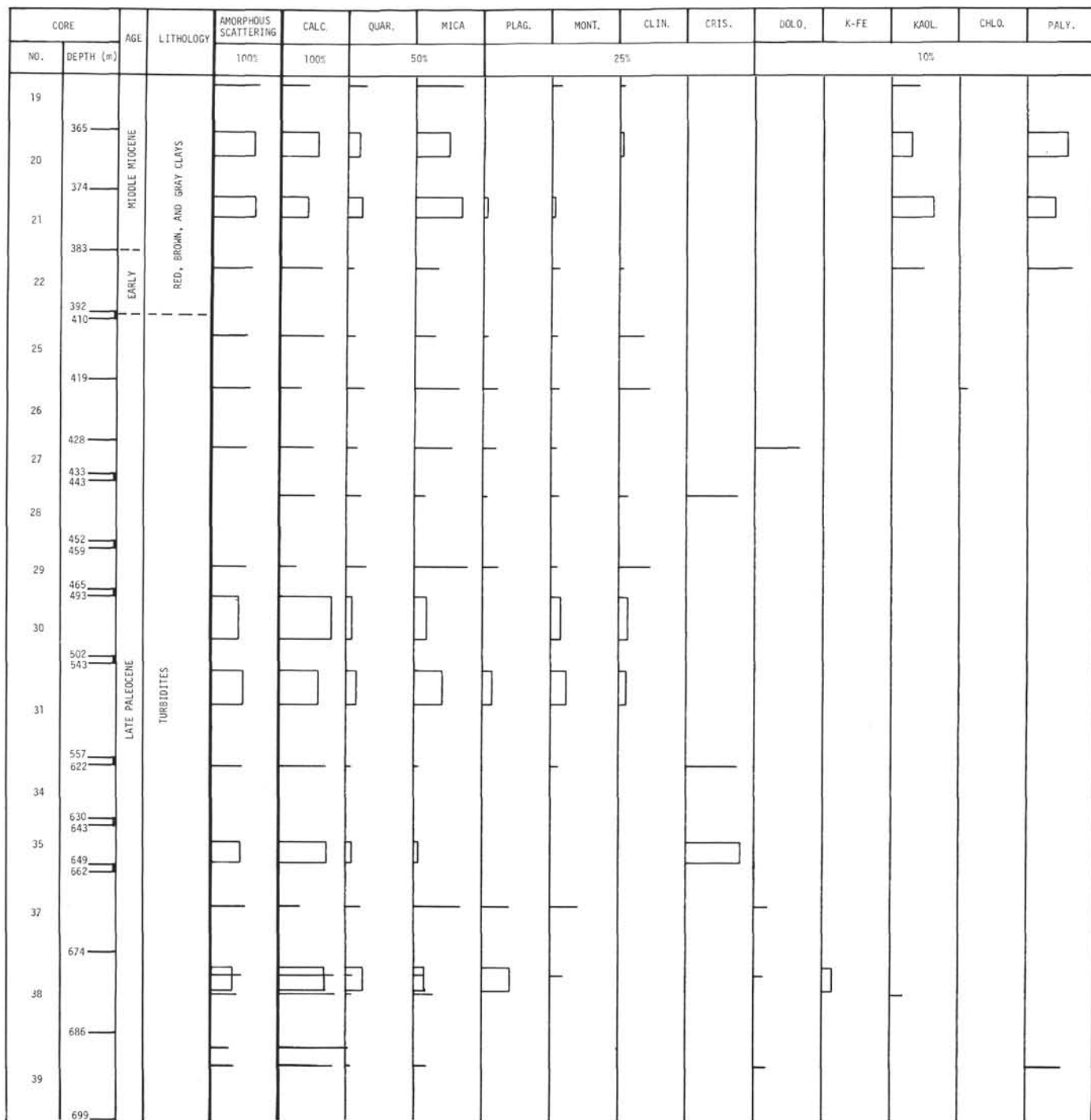


Figure 21. (Continued)

(4) The Bay of Biscay Suite (Sites 118 and 119) is characterized by high concentrations of quartz and mica but differs from other North Atlantic sediments in containing very low plagioclase and chlorite concentrations. The sediments at Sites 118 and 119 resemble the sediments from the eastern abyssal plane of the Bay of Biscay (described by Nesteroff *et al.*, 1968) with respect to the mineral assemblages as well as the high content of well-crystallized mica. Nesteroff *et al.* have ascribed the

source of these sediments to local terrigenous detrital sources.

A sudden increase in the kaolinite content in Eocene time is noted at Site 119 (Figure 21). This increase coincides in time with the last opening of the Bay of Biscay (Jones and Ewing, 1969) as well as the Pyrenean phase of the Alpine Orogeny (Rutten, 1969) and may be a reflection of an increased flux of sediments resulting from the uplift of the Pyrenees (Y. Lancelot, personal communication).

REFERENCES

- Boer, Jelle De, Schilling, Jean-Guy and Krause, D. C., 1969. Magnetic polarity of pillow basalts from Reykjanes Ride. *Science*. **166**, 966.
- Jacobs, M. B., 1970. Clay mineral investigations of Cretaceous and Quaternary deep sea sediments of the North American basin. *J. Sediment. Petrol.* **40**, 864.
- Johnson, G. L. and Schneider, E. D., 1969. Depositional ridges in the North Atlantic. *Earth Planet. Sci. Letters*. **6**, 416.
- Jones, E. J. W. and Ewing, J. I., 1969. Age of the Bay of Biscay: Evidence from seismic profiles and bottom samples. *Science*. **166**, 102.
- Jones, E. J. W. and Funnell, B. M., 1968. Association of a seismic reflection and Upper Cretaceous sediments in the Bay of Biscay. *Deep Sea Res.* **15**, 701.
- Marlowe, J. I., 1969. A succession of Tertiary strata off Nova Scotia, as determined by dredging. *Canadian J. Earth Sci.* **6**, 1077.
- Nesteroff, W. D., Duplaix, S., Sauvage, J., Lancelot, Y., Melieres F. and Vincent, E., 1968. Les depots recents du canyon de Cap-Breton. *Bull. Soc. Geol. France*. **10** (7). 218.
- Palmer, A. R., 1969. Cambrian trilobite distributions in North America and their bearing on Cambrian paleogeography of Newfoundland. In *North Atlantic - Geology and Continental Drift. A Symposium*. M. Kay (Ed.). Tulsa (Am. Assoc. Petrol. Geol.), 139.
- Phipps, C. V. G. and King, L. H., 1969. Chemical, mineralogical and textural variations in sediments from the Scotian Shelf. *Maritime Sediments*. **5**, 101.
- Rutten, M. G., 1969. *The Geology of Western Europe*. Amsterdam (Elsevier Publishing Co.), 520 pp.
- Zemmels, I., Cook, H. E. and Hathaway, J. C., 1972. X-ray mineralogy studies, Leg 11. In Hollister, C. D. *et al.*, 1972. *Initial Reports of the Deep Sea Drilling Project, Volume XI*. Washington (U. S. Government Printing Office), in press.

TABLE 1
Results of X-ray Diffraction Analyses from Site 111

Hole 111: Bulk Samples

Core	Depth	Sample Depth	Diff.	Amorphous	Calc.	Dolo.	Quar.	K-Fe.	Plag.	Kaol.	Mica	Chlo.	Mont.	Clin.	Amph.
1	0-5	4.55-4.55	66.6	47.8	27.7	11.8	25.1	—	21.4	2.4	8.7	—	—	—	2.8
2	94-103	98.00-101.00	69.7	52.6	4.4	7.7	38.3	4.4	13.1	2.5	23.1	2.7	1.7	—	2.0
3	189-198	191.50-191.50	69.3	52.0	39.4	—	33.3	—	4.2	—	21.3	—	1.9	—	—

Hole 111A: Bulk Samples

Core	Depth	Sample Depth	Diff.	Amorphous	Calc.	Dolo.	Quar.	K-Fe.	Plag.	Kaol.	Mica	Chlo.	Mont.	Clin.	Amph.
1	105-114	106.09-113.50	72.6	57.2	6.7	6.1	38.0	—	15.2	1.3	24.6	3.4	2.5	—	2.2
2	114-120	114.99-119.48	76.1	62.7	7.2	3.8	41.1	—	12.6	4.3	23.6	2.2	5.2	—	—
3	120-125	122.00-124.50	73.9	59.2	1.5	5.1	41.0	2.7	10.4	—	30.4	2.9	6.0	—	—
4	125-134	126.00-126.00	68.6	50.9	—	5.6	44.9	—	11.7	4.0	28.8	2.7	2.3	—	—
		127.00-127.00	67.0	48.4	36.0	2.0	29.6	7.9	14.2	2.3	6.7	—	—	—	1.4
		127.50-127.50	71.9	56.2	—	2.5	38.7	4.8	14.5	3.7	24.8	2.4	7.0	—	1.6
5	134-143	139.66-140.23	77.5	64.9	—	2.0	38.2	5.3	12.3	4.6	24.8	2.3	10.6	—	—
6	143-152	144.00-144.00	71.6	55.6	—	2.1	40.9	3.5	13.0	4.5	27.1	1.9	7.2	—	—
		145.50-145.50	73.0	57.7	38.9	—	26.8	4.6	10.2	1.6	9.5	—	8.4	—	—
		146.70-146.70	77.8	65.3	83.7	—	5.4	—	—	1.3	4.8	—	4.7	—	—
		146.95-146.95	86.4	78.7	38.2	—	17.9	—	—	2.6	15.1	—	10.3	15.9	—
		147.01-147.01	89.4	83.4	—	—	24.4	—	2.4	8.8	23.5	—	36.7 ¹	4.2	—
		147.14-147.14	81.5	71.1	37.5	—	16.0	—	2.3	2.9	14.5	—	6.7	20.1	—
		147.18-147.18	90.7	85.5	—	—	23.0	—	—	12.4	24.4	—	30.5 ¹	9.7	—
		147.26-147.26	84.9	76.4	41.5	—	20.1	—	6.6	5.9	24.5	—	—	1.4	—
7	152-161	157.90-160.93	89.7	83.9	38.0	—	14.5	—	1.3	5.3	19.4	—	15.5 ¹	6.0	—
8	161-164	162.19-163.65	80.2	69.1	46.3	—	6.3	—	—	—	10.0	—	34.0	3.4	—
9	164-173	165.00-165.00	78.6	66.5	46.0	—	5.0	—	—	—	8.8	—	37.3	2.8	—
10	173-182	174.24-177.65	83.2	73.7	66.9	—	9.8	—	—	—	11.1	—	—	12.2	—
11	182-190	183.50-183.50	54.1	28.3	98.2	—	0.5	1.3	—	—	—	—	—	—	—
		185.00-185.00	54.6	29.0	97.8	—	0.7	1.5	—	—	—	—	—	—	—
		186.50-186.50	55.3	30.2	99.4	—	—	—	—	—	—	—	—	—	—
		187.00-187.00	52.6	26.0	99.5	—	0.5	—	—	—	—	—	—	—	—
		188.00-188.00	56.6	32.2	98.0	—	0.7	1.3	—	—	—	—	—	—	—
		189.50-189.50	58.2	34.7	97.0	—	0.9	2.1	—	—	—	—	—	—	—

TABLE 2
Results of X-Ray Diffraction Analyses from Site 112

Hole 112: Bulk Samples														
Core	Depth	Sample Depth	Diff.	Amorphous	Calc.	Dolo.	Quar.	Plag.	Kaol.	Mica	Chlo.	Mont.	Hema.	Amph.
1	28-37	35.50-35.50	76.1	62.6	31.5	6.5	17.4	17.1	2.1	19.4	1.4	—	—	4.6
2	100-109	106.00-108.50	78.7	66.8	27.8	1.6	26.4	12.4	3.0	18.5	1.3	7.3	—	1.7
3	150-159	152.49-158.98	77.1	64.3	40.2	—	21.1	7.5	5.4	16.5	—	9.3	—	—
4	200-209	201.50-202.50	82.1	72.1	31.8	—	20.6	7.2	8.8	19.1	—	12.6	—	—
5	270-279	271.00-278.51	83.1	73.6	25.8	—	21.6	9.4	2.3	19.0	1.9	20.0	—	—
6	279-288	284.50-284.50	80.5	69.5	36.1	—	15.2	4.8	5.0	16.1	—	22.8	—	—
7	288-297	290.51-290.51	79.0	67.2	36.3	—	16.8	8.8	4.8	16.8	—	16.6	—	—
9	306-315	307.40-310.60	84.0	75.0	10.3	—	20.7	10.3	—	22.7	2.7	33.2	—	—
11	324-333	325.00-329.51	73.9	59.3	55.1	—	8.2	1.8	—	11.1	—	23.8	—	—
12	383-393	383.95-385.85	72.9	57.6	45.4	—	13.3	—	—	17.6	—	23.7	—	—
13	441-450	443.50-448.00	75.6	61.9	35.7	—	18.4	—	—	14.5	—	31.5	—	—
14	499-508	499.50-503.99	73.8	59.1	40.6	—	23.4	—	—	10.7	—	25.3	—	—
16	652-659	653.00-653.00	76.2	62.9	1.7	—	79.8	—	—	7.5	—	3.0	7.9	—

Hole 112A: Bulk Samples														
Core	Depth	Sample Depth	Diff.	Amorphous	Calc.	Dolo.	Quar.	Plag.	Kaol.	Mica	Chlo.	Mont.	Hema.	Amph.
1	79-88	85.00-85.00	77.9	65.5	3.3	6.0	34.8	19.4	4.3	22.2	2.6	4.3	—	3.1
3	97-106	100.00-100.00	80.5	69.6	3.0	4.5	34.5	17.1	5.7	24.5	1.7	7.0	—	2.1

TABLE 3
Results of X-ray Diffraction Analyses From Site 113

Hole 113: Bulk Samples															
Core	Depth	Sample Depth	Diff.	Amorphous	Calc.	Dolo.	Quar.	Plag.	Kaol.	Mica	Chlo.	Mont.	Clin.	Augi.	Amph.
1	50-59	54.00-57.01	81.2	70.6	25.1	4.4	15.4	20.0	2.6	21.7	1.1	-	-	6.3	3.4
2	99-108	102.00-103.35	81.9	71.8	2.6	1.3	18.6	33.6	3.1	19.6	1.6	3.0	-	10.3	6.4
3	156-165	158.50-160.07	78.8	66.9	8.7	2.1	18.6	29.9	2.8	17.2	1.3	3.4	-	11.5	4.4
4	204-207	205.28-206.31	77.1	64.2	-	-	18.5	34.9	1.6	15.2	1.5	4.3	-	19.6	4.4
5	254-257	255.16-255.17	65.5	46.1	1.9	-	31.7	50.0	-	6.8	-	-	-	4.6	5.0
7	549-558	550.47-550.47	78.7	66.7	3.1	-	16.4	28.1	-	27.9	4.7	15.0	-	-	4.8
		550.97-550.97	80.9	70.1	18.0	-	16.6	29.1	2.1	23.8	1.7	4.1	1.9	-	2.6
		551.03-551.03	81.8	71.6	20.9	-	17.6	19.3	2.3	22.9	1.7	10.7	2.0	-	2.6
		551.23-551.23	84.3	75.5	-	-	22.6	12.5	7.8	24.6	1.8	29.2	-	-	1.5
8	663-669	663.27-666.05	79.1	67.4	3.0	-	21.7	21.2	2.9	27.8	2.3	14.2	3.0	-	3.8
9	710-715	712.70-714.20	80.8	69.9	-	-	22.1	17.8	3.6	34.3	3.9	13.0	3.4	-	1.9
10	759-766	766.00-766.00	79.4	67.9	3.9	-	25.3	19.1	-	26.1	2.0	20.2	1.8	-	1.6
11	810-815	811.58-812.07	71.7	55.8	1.5	-	13.3	22.7	2.1	9.9	-	47.3	-	-	3.2

TABLE 4
Results of X-ray Diffraction Analyses from Site 114.

Hole 114: Bulk Samples													
Core	Depth	Sample Depth	Diff.	Amorphous	Calc.	Quar.	Plag.	Kaol.	Mica	Chlo.	Mont.	Pyri.	Augi.
2	200-209	202.50-208.51	84.8	76.3	24.3	6.6	25.0	-	4.3	3.7	3.1	-	33.1
3	300-309	302.50-307.40	88.3	81.8	30.3	2.1	22.3	1.0	-	-	-	1.8	42.5
4	400-409	401.68-408.58	86.0	78.1	28.9	1.4	35.3	-	-	-	-	2.0	32.5
5	499-509	499.95-507.71	80.7	69.8	75.1	1.2	11.2	-	-	-	-	-	12.5
		508.97-508.97	84.9	76.4	50.0	1.1	21.5	-	-	-	-	-	23.6
6	600-609	600.17-607.85	84.0	75.0	54.3	3.4	16.8	1.6	-	-	2.7	1.8	19.4

TABLE 5
Results of X-ray Diffraction Analyses from Site 115

Hole 115: Bulk Sample									
Core	Depth	Sample Depth	Diff.	Amorphous	Quar.	Plag.	Kaol.	Augi.	Anal.
4	100-107	101.70-101.70	82.9	73.3	6.3	42.3	4.3	47.0	P*

*P = Present.

TABLE 6
Results of X-ray Diffraction Analyses from Site 116

Hole 116: Bulk Samples										
Core	Depth	Sample Depth	Diff.	Amorphous	Calc.	Quar.	Cris.	Mica	Mont.	Clin.
1	70-79	71.00-77.01	55.7	30.8	99.5	0.5	—	—	—	—
2	109-118	110.00-115.06	53.3	27.0	100.0	—	—	—	—	—
3	159-168	160.00-165.09	53.3	27.0	100.0	—	—	—	—	—
4	209-218	210.99-216.59	50.7	22.9	100.0	—	—	—	—	—
5	259-268	259.42-266.60	53.9	27.9	100.0	—	—	—	—	—
6	309-318	209.99-313.59	53.8	27.8	99.6	0.4	—	—	—	—
7	359-368	360-362.06	52.0	24.9	100.0	—	—	—	—	—
8	409-418	411.17-412.05	52.2	25.4	100.0	—	—	—	—	—
9	459-468	460.50-463.00	51.5	24.2	100.0	—	—	—	—	—
10	509-518	517.53-517.53	56.7	32.3	100.0	—	—	—	—	—
11	559-568	567.27-567.27	59.9	37.3	95.4	0.5	4.1	—	—	—
12	599-608	600.00-600.00	55.0	29.7	98.9	—	—	—	1.1	—
15	662-671	662.73-669.53	55.6	30.7	98.7	0.1	—	1.2	—	—
16	671-680	673.30-673.30	59.4	36.5	100.0	—	—	—	—	—
17	680-689	685.50-688.60	56.0	31.3	100.0	—	—	—	—	—
20	701-710	701.45-709.60	61.2	39.3	95.9	0.5	—	—	3.6	—
21	710-719	715.10-715.10	59.0	36.0	90.1	—	9.9	—	—	—
22	719-728	727.74-727.74	55.1	29.9	95.4	0.5	3.0	—	—	1.1
23	750-759	758.62-758.84	56.0	31.2	92.1	2.6	3.9	—	—	1.4
26	825-831	826.50-826.50	59.0	35.9	95.1	0.5	—	—	1.8	2.6
27	831-840	834.00-834.00	60.3	38.0	89.6	—	10.4	—	—	—

Hole 116: 2-20 μ m Fractions

Core	Depth	Sample Depth	Diff.	Amorphous	Quar.	Cris.	Plag.	Kaol.	Mica	Mont.	Clin.	Phil.	Pyri	Algi.	Cele.	Bari.
1	70-79	70-05-70-05	90.5	85.1	35.2	—	31.1	—	11.2	—	—	11.9	—	10.5	—	—
3	159-168	159.31-158.31	92.4	88.2	47.1	—	29.0	—	16.7	—	—	—	7.2	—	—	—
7	359-368	359.09-359.09	91.5	86.7	61.8	—	18.0	—	17.8	—	—	—	2.5	—	—	—
8	409-418	410.81-410.81	91.2	86.3	47.4	—	29.4	—	20.0	—	—	—	3.2	—	—	—
9	459-468	459.08-459.03	48.9	20.2	—	—	—	—	—	—	—	—	—	—	100.0	—
11	559-568	561.56-561.56	69.9	53.0	16.3	15.3	3.9	—	—	—	55.2	—	1.4	—	—	—
		561.61-561.61	75.2	61.3	4.7	79.7	—	—	—	—	13.8	—	1.8	—	—	—
12	599-608	599.38-599.38	92.4	88.1	37.1	—	12.6	3.7	19.1	15.5	—	—	6.6	—	—	5.1

TABLE 6 – Continued

Core	Depth	Sample Depth	Diff.	Amorphous	Quar.	Cris.	Plag.	Kaol.	Mica	Mont.	Clin.	Phil.	Pyri	Algi.	Cele.	Bari.
15	662-671	665.20-665.20	94.8	91.8	51.6	–	20.7	–	16.8	–	–	–	10.9	–	–	–
		671.00-671.00	97.5	96.0	55.3	–	10.0	–	22.0	–	–	–	12.7	–	–	–
16	671-680	672.91-672.91	96.4	94.3	50.5	–	15.4	–	26.2	–	–	–	7.9	–	–	–
17	680-689	684.66-684.66	96.6	94.7	56.1	–	18.0	–	19.2	–	–	–	6.6	–	–	–
20	701-710	707.55-707.55	74.7	60.4	17.6	17.4	18.6	–	9.2	–	24.3	–	10.8	–	–	2.1
21	710-719	713.23-713.23	71.2	55.1	22.1	29.3	8.8	1.4	9.5	–	26.3	–	2.5	–	–	–
22	719-728	726.67-726.67	69.7	52.7	10.3	55.9	3.3	–	5.0	–	23.9	–	1.7	–	–	–
23	750-759	753.53-753.53	76.0	62.5	11.9	34.9	12.5	–	4.2	–	31.4	–	5.0	–	–	–
26	825-831	828.01-828.01	66.3	47.4	6.3	31.9	8.6	–	3.7	–	46.3	–	3.2	–	–	–

Hole 116: <2 μm Fractions

Core	Depth	Sample Depth	Diff.	Amorphous	Quar.	Cris.	K-Fe.	Plag.	Kaol.	Mica	Mont.	Clin.	Pyri	Gyps.	Apat.	Cele.	Hali.
1	70-79	70.05-70.05	94.0	90.6	18.4	–	–	13.2	12.2	36.2	19.2 ²	–	–	–	–	–	–
2	109-118	109.21-109.21	87.8	80.9	19.0	–	–	6.5	13.2	35.1	21.0 ¹	–	–	–	5.3	–	–
3	159-168	159.31-159.31	88.6	82.1	15.2	–	5.6	7.0	15.3	27.5	27.5	–	2.0	–	–	–	–
5	259-268	259.07-259.07	87.8	80.9	20.1	–	–	6.1	12.6	22.7	38.4	–	–	–	–	–	–
6	309-318	309.21-309.21	94.3	91.1	17.6	–	–	5.7	15.5	47.5	13.7	–	–	–	–	–	–
7	359-368	359.09-359.09	97.5	96.2	21.4	–	17.2	6.1	8.6	25.1	21.4	–	–	–	–	–	–
8	409-418	410.81-410.81	89.9	84.2	25.5	–	19.5	2.9	13.2	38.9	–	–	–	–	–	–	–
9	459-468	459.03-459.03	90.2	84.7	7.0	–	–	–	5.2	23.5	15.0	–	–	–	–	–	–
10	509-518	509.86-509.86	85.2	76.9	14.8	–	–	3.5	5.3	18.8	55.2	–	2.3	–	–	–	–
11	559-568	561.56-561.56	91.6	86.9	7.2	26.5	–	–	–	21.7	20.3	3.4	–	–	–	–	20.9
		567.61-567.61	83.2	73.7	1.7	55.3	–	–	–	3.5	–	2.1	–	–	34.3	–	3.1
12	599-608	599.38-599.38	88.1	81.3	9.0	–	–	–	–	14.6	43.4	–	–	2.1	–	–	30.8
15	662-671	665.20-665.20	93.0	89.1	10.9	–	–	–	–	14.2	39.2	–	–	4.2	–	–	31.3
		671.00-671.00	92.5	88.3	11.1	–	–	–	–	14.7	40.8	–	–	4.3	–	–	29.0
16	671-680	672.91-672.91	94.6	91.6	12.4	–	–	–	–	23.6	64.0	–	–	–	–	–	–
17	680-689	684.66-684.66	95.8	93.7	8.4	–	–	–	–	20.6	70.9	–	–	–	–	–	–
20	701-710	707.55-707.55	84.9	76.4	3.9	5.8	–	5.2	–	6.5	76.5	–	–	–	–	–	2.1
21	710-719	713.23-713.23	84.2	75.2	4.9	74.5	–	–	–	4.4	13.3	1.8	–	–	–	–	1.1
22	719-728	726.67-726.67	82.9	73.3	2.1	92.0	–	–	–	2.4	2.8	–	–	–	–	–	–
23	750-759	756.53-756.53	83.9	74.9	6.1	48.2	–	–	–	11.3	25.8	7.1	–	–	–	–	1.5
26	825-831	828.01-828.01	80.6	69.6	2.7	55.1	–	1.6	–	3.7	33.1	1.9	1.8	–	–	–	–
27	831-840	832.50-832.50	81.2	70.6	2.8	46.8	–	1.6	–	4.0	42.7	–	2.1	–	–	–	–

¹See text.²See text.

TABLE 6 – Continued

Hole 116A: Bulk Samples															
Core	Depth	Sample Depth	Diff.	Amorphous	Calc.	Dolo.	Quar.	K-Fe.	Plag.	Kaol.	Mica	Chlo.	Mont.		
1	0-9	0.81-0.81	61.4	39.7	93.0	–	2.8	–	2.3	–	1.9	–	–		
2	9-18	11.50-15.10	71.8	56.0	45.8	6.0	21.1	–	13.1	1.3	11.3	1.4	–		
3	18-27	24.00-25.00	54.6	29.0	99.5	–	0.5	–	–	–	–	–	–		
4	27-36	29.49-34.60	67.7	49.5	76.2	–	10.5	–	3.7	–	8.5	1.1	–		
5	36-45	38.50-40.01	67.1	48.7	82.1	–	–	1.8	3.6	–	5.0	–	–		
6	45-54	52.54-52.54	59.8	37.1	92.3	–	2.8	1.4	1.2	–	2.3	–	–		
7	54-63	56.50-59.51	64.5	44.5	80.9	–	7.4	1.7	3.5	–	5.2	–	1.3		
		62.50-62.50	75.3	61.4	35.3	–	31.3	–	10.8	2.0	14.0	2.4	4.2		
8	63-72	65.46-70.58	57.7	33.9	96.1	–	0.9	–	3.0	–	–	–	–		
9	72-81	73.00-73.00	58.2	34.7	99.5	–	0.5	–	–	–	–	–	–		
10	81-90	88.54-88.54	53.2	26.9	100.0	–	–	–	–	–	–	–	–		
11	90-99	91.00-91.00	53.7	27.7	100.0	–	–	–	–	–	–	–	–		
Hole 116A: 2-20 μ m Fractions															
Core	Depth	Sample Depth	Diff.	Amorphous	Quar.	K-Fe.	Plag.	Kaol.	Mica	Chlo.	Clin.	Phil.	Pyri.	Amph.	Augi.
1	0-9	1.61-1.61	67.9	49.8	47.3	–	28.5	–	16.8	3.0	–	–	–	1.6	2.7
2	9-18	13.51-13.51	61.6	40.1	31.6	6.5	17.7	1.6	36.5	2.5	–	–	–	1.2	2.4
3	18-27	18.13-18.13	75.5	61.7	41.9	–	31.0	–	16.4	3.4	1.3	–	–	–	6.0
4	27-36	28.52-28.52	57.7	34.0	41.0	7.6	19.6	–	25.1	4.5	–	–	–	2.2	–
5	36-45	39.01-39.01	65.4	46.0	41.8	3.3	21.1	1.4	26.6	4.2	–	–	–	1.6	–
6	45-54	48.01-48.01	70.5	53.9	38.9	12.3	23.7	–	19.8	3.5	–	–	–	2.0	–
7	54-63	55.51-55.51	78.5	66.4	46.1	–	27.9	1.4	17.7	2.8	–	–	–	–	4.1
8	63-72	70.62-70.62	77.2	64.4	43.7	–	28.6	–	13.3	3.3	–	–	–	–	11.1
9	72-81	73.25-73.25	66.4	47.5	39.5	7.1	18.9	–	26.9	7.6	–	–	–	–	–
10	81-90	84.01-84.01	92.6	88.4	30.8	–	29.4	–	18.5	–	–	13.1	3.3	–	4.9
11	90-99	90.20-90.20	87.0	79.4	48.6	–	19.4	–	–	–	1.8	12.5	–	–	–
Hole 116A: <2 μ m Fractions															
Core	Depth	Sample Depth	Diff.	Amorphous	Quar.	K-Fe.	Plag.	Kaol.	Mica	Chlo.	Mont.	Pyri.	Apat.		
1	0-9	1.61-1.61	88.4	81.9	18.9	–	6.6	8.2	33.9	3.8	19.1	–	9.4		
2	9-18	13.51-13.51	82.2	72.2	24.3	–	8.5	–	43.4	7.2	16.6 ²	–	–		
3	18-27	18.13-18.13	84.3	75.5	21.9	5.5	9.1	8.1	36.4	4.3	14.7	–	–		
4	27-36	28.53-28.53	82.1	72.0	29.3	–	13.6	11.8	35.6	–	9.7	–	–		

²See text.

TABLE 6 – Continued

Core	Depth	Sample Depth	Diff.	Amorphous	Quar.	K-Fe	Plag.	Kaol.	Mica	Chlo.	Mont.	Pyri.	Apat.
5	36-45	39.01-39.01	87.5	80.4	12.9	5.7	6.1	14.6	27.0	–	33.7	–	–
6	45-54	48.01-48.01	84.3	75.5	14.0	–	5.3	7.1	32.1	3.6	28.8	–	9.1
7	54-63	55.51-55.51	85.4	77.2	15.6	–	7.9	9.3	32.8	3.5	31.0	–	–
8	63-72	70.62-70.62	87.3	80.1	18.1	–	8.4	7.7	27.1	4.5	34.2	–	–
9	72-81	73.25-73.25	76.9	63.9	16.5	–	6.0	11.1	29.5	4.3	32.7	–	–
10	81-90	84.01-84.01	91.1	86.0	14.9	–	5.8	–	30.9	7.1	23.2	4.0	14.0
11	90-99	90.20-90.20	92.9	89.0	15.6	–	4.4	2.9	31.7	3.3	–	2.3	39.8

TABLE 7
Results of X-ray Diffraction Analyses From Site 117

Hole 117: Bulk Samples														
Core	Depth	Sample Depth	Diff.	Amorphous	Calc.	Quar.	Clin.							
2	100-109	104.01-104.01	58.6	35.3	98.3	0.3	1.4							
Hole 117: 2-20 μm Fraction														
Core	Depth	Sample Depth	Diff.	Amorphous	Quar.	K-Fe.	Plag.	Mica	Clin.	Anal.				
2	100-109	104.58-104.58	67.5	49.2	6.4	3.3	3.8	2.5	83.8	P*				
*P = Present.														
Hole 117: <2 μm Fraction														
Core	Depth	Sample Depth	Diff.	Amorphous	Quar.	Mica	Mont.	Clin.						
2	100-109	104.58-104.58	92.5	88.2	3.1	37.5	46.6	12.7						
Hole 117A: Bulk Samples														
Core	Depth	Sample Depth	Diff.	Amorphous	Calc.	Quar.	K-Fe.	Plag.	Kaol.	Mont.	Clin.	Augi.		
1	146-155	146.75-146.75	82.9	73.3	13.4	2.3	—	19.7	—	40.0	19.9	4.7		
3	222-227	222.00-227.00	85.4	77.2	30.9	1.0	10.0	2.4	2.7	53.0	—	—		
4	270-272	270.00-272.00	80.8	70.0	37.2	1.0	2.2	1.3	—	45.8	12.5	—		
6	276-285	282.64-282.64	80.9	70.2	30.3	1.8	—	7.3	—	48.7	11.9	—		
Hole 117A: 2-20 μm Fractions														
Core	Depth	Sample Depth	Diff.	Amorphous	Quar.	Cris.	K-Fe.	Plag.	Kaol.	Mont.	Clin.	Magn.	Pyri.	Bari.
1	146-155	146.67-146.67	69.1	51.7	6.4	25.3	24.0	40.7	—	3.7	—	—	—	—
4	270-272	270.00-272.00	67.3	48.9	1.8	—	21.3	50.1	9.6 ¹	6.8	1.3	—	—	—
6	276-285	282.64-282.64	71.5	55.4	2.8	—	45.9	28.8	—	5.1	3.3	14.2	—	—
¹ See text.														
Hole 117A: <2 μm Fractions														
Core	Depth	Sample Depth	Diff.	Amorphous	Quar.	Cris.	K-Fe.	Plag.	Kaol.	Mont.	Clin.	Pyri.	Hali.	Anat.
1	146-155	146.67-146.67	82.7	72.7	3.8	40.8	—	4.0	—	47.1 ¹	4.3	—	—	—
3	222-227	222.91-222.91	79.3	67.6	3.0	—	6.7	—	2.6	84.8 ¹	—	1.3	—	1.5
4	270-272	270.00-272.00	78.3	66.2	1.0	—	4.3	—	—	81.5 ¹	9.8	—	3.4	—
6	276-285	281.61-281.61	77.8	65.4	1.2	—	9.4	—	—	82.0 ¹	2.2	1.4	3.8	—
¹ See text.														

TABLE 8
Results of X-ray Diffraction Analyses From Site 118

Hole 118: Bulk Samples																
Core	Depth	Sample Depth	Diff.	Amorphous	Calc.	Dolo.	Arag.	Side	Quar.	K-Fe	Plag.	Kaol.	Mica	Chlo.	Mont.	Clin.
1	96-105	98.40-103.58	72.2	56.6	54.4	—	—	—	22.8	—	5.8	5.6	6.8	4.5	—	—
		104.15-104.15	62.7	41.7	81.3	—	—	—	6.8	—	—	—	11.9	—	—	—
2	200-209	201.74-208.51	71.0	54.6	19.2	—	—	—	32.0	—	1.9	3.3	40.5	3.1	—	—
3	300-309	302.58-303.08	73.6	58.8	29.2	—	—	1.5	30.6	—	1.3	9.6	27.7	—	—	—
4	350-359	352.50-353.10	66.0	46.8	26.3	—	—	—	42.2	2.6	8.1	—	18.5	1.1	1.1	—
5	399-409	401.13-402.10	73.3	58.3	32.0	—	—	—	16.8	—	1.7	6.2	41.9	1.2	—	—
6	448-457	448.00-449.35	74.3	59.8	47.8	—	13.7	—	14.3	—	—	2.0	19.0	1.1	2.1	—
7	496-501	496.95-496.95	61.7	40.1	86.8	4.3	1.7	—	7.2	—	—	—	—	—	—	—
8	505-512	505.57-505.57	60.6	38.5	94.4	2.2	—	—	1.9	—	—	—	—	—	1.5	—
9	553-559	555.90-555.90	75.6	61.9	41.4	—	—	—	18.3	—	2.5	4.1	23.9	—	9.8	—
10	604-613	604.89-604.89	70.8	54.4	35.2	1.3	—	—	29.9	—	2.3	3.7	24.3	—	3.3	—
11	650-658	650.23-650.23	73.9	59.2	—	—	—	—	30.3	—	3.5	6.3	56.8	—	3.2	—
13	693-695	695.00-695.00	68.7	51.1	78.1	—	—	—	5.3	—	—	1.9	11.1	—	3.6	—
15	714-723	714.00-715.50	66.6	47.8	80.9	—	—	—	4.4	—	—	2.2	12.6	—	0.0	—
16	723-732	723.10-723.10	83.3	73.9	—	—	—	—	19.2	—	4.3	9.8	42.9	0.0	6.8 ¹	17.1
17	732-741	733.03-733.03	89.2	83.1	—	—	—	—	33.1	12.2	4.1	10.6	40.0	—	—	—
18	750-756	750.20-750.20	81.9	71.8	—	—	—	—	60.2	—	3.8	18.5	13.8	—	3.8 ¹	—

¹ See text.

TABLE 9
Results of X-ray Diffraction Analyses From Site 119

Hole 119: Bulk Samples																
Core	Depth	Sample Depth	Diff.	Amorphous	Calc.	Dolo.	Quar.	K-Fe	Plag.	Kaol.	Mica	Chlo.	Mont.	Paly.	Clin.	Cris.
1	10-19	11.85-11.85	75.5	61.7	28.6	3.3	24.3	—	4.5	3.7	31.5	1.8	2.4	—	—	—
2	50-59	51.55-51.55	69.9	53.0	27.6	—	23.2	—	2.7	3.9	39.5	3.1	—	—	—	—
		52.45-52.45	65.6	46.2	76.5	—	7.4	—	—	1.1	15.1	—	—	—	—	—
3	100-109	100.50-101.58	0.0	0.0	73.9	—	7.5	—	—	1.1	17.5	—	—	—	—	—
4	150-159	151.00-151.55	74.5	60.1	54.3	—	15.1	—	—	4.5	26.1	—	—	—	—	—
5	198-207	199.50-200.51	64.9	45.2	72.2	—	6.7	—	—	2.5	17.0	—	1.5	—	—	—
6	240-249	242.50-243.06	72.1	56.5	58.9	—	10.4	—	—	3.5	22.1	—	5.2	—	—	—
7	249-258	251.50-251.50	74.5	60.2	37.1	—	12.5	—	1.4	7.4	31.0	—	10.5	—	—	—
8	258-267	258.80-263.51	77.2	64.4	24.2	—	19.0	—	2.1	6.5	38.6	—	9.6	—	—	—
		267-276	268.65-268.65	80.1	69.0	15.5	—	24.2	—	3.8	6.9	35.2	—	14.4	—	—
10	276-284	269.18-269.18	79.2	67.4	—	—	25.6	—	3.2	7.7	47.7	—	15.9	—	—	—
		276.98-276.98	69.3	52.0	55.2	—	11.0	—	1.5	3.4	23.3	—	5.6	—	—	—
		277.50-277.50	70.0	53.2	52.1	—	9.7	—	—	5.0	30.1	—	3.2	—	—	—
		278.50-278.50	74.2	59.6	43.4	—	13.4	—	1.6	5.0	29.8	—	6.7	—	—	—
11	284-293	285.00-285.00	66.8	48.1	70.5	—	7.5	—	—	2.6	16.4	—	3.0	—	—	—
12	293-302	293.78-296.67	70.6	54.1	60.1	—	9.6	—	1.3	3.5	23.6	—	1.8	—	—	—
13	302-311	304.50-306.51	64.7	44.8	79.0	—	6.1	—	—	1.8	11.9	—	—	—	1.2	—
14	311-320	311.83-317.52	66.6	47.8	73.2	—	7.1	—	—	2.3	16.0	—	—	—	1.3	—
15	320-329	321.03-327.12	63.7	43.2	81.0	—	5.9	—	—	1.6	9.9	—	—	—	1.6	—
16	329-338	330.00-333.54	70.9	54.6	69.6	—	8.8	—	—	2.6	17.2	—	—	—	1.8	—
17	338-347	338.10-343.41	71.4	55.4	65.5	—	11.1	—	—	2.1	18.4	—	—	—	2.9	—
18	347-356	348.50-355.51	67.0	48.4	79.7	—	5.7	—	—	1.1	12.2	—	—	—	1.3	—
19	356-365	358.50-358.50	80.1	68.9	42.5	—	13.5	—	—	4.1	34.6	—	3.5	—	1.9	—
20	365-374	365.40-369.00	75.7	62.0	56.6	—	8.8	—	—	3.0	24.5	—	—	5.9	1.2	—
21	374-383	375.00-378.02	76.7	63.7	41.9	—	11.0	—	1.4	6.2	34.0	—	1.3	4.1	—	—
22	383-392	385.50-385.50	74.2	59.7	62.8	—	4.8	—	—	4.7	16.9	—	2.9	6.5	1.4	—
25	410-419	412.50-412.50	70.0	53.1	66.1	—	5.9	—	1.7	—	14.8	—	2.2 ¹	—	9.2	—
26	419-428	420.18-420.18	72.7	57.4	33.4	—	12.9	—	5.4	—	32.6	1.2	3.0 ¹	—	11.6	—
27	428-433	429.00-429.00	69.2	51.9	51.3	6.5	8.1	—	4.9	—	27.3	—	2.0 ¹	—	—	—
28	443-452	445.10-445.10	0.0	0.0	54.1	—	10.9	—	1.6	—	8.1	—	3.0	—	3.4	18.8
29	459-465	461.53-461.53	69.6	52.5	26.4	—	14.8	—	5.7	—	39.0	—	2.4	—	11.8	—
30	493-502	493.00-499.31	62.6	41.6	79.1	—	4.6	—	—	—	9.2	—	3.8 ¹	—	3.4	—

¹See text.

TABLE 9 – Continued

Core	Depth	Sample Depth	Diff.	Amorphous	Calc.	Dolo.	Quar.	K-Fe	Plag.	Kaol.	Mica	Chlo.	Mont.	Paly.	Clin.	Cris.
31	543-557	543.98-548.98	66.7	48.0	59.4	–	7.8	–	3.6	–	20.7	–	5.7 ¹	–	2.8	–
34	622-630	622.18-622.20	66.0	46.9	70.8	–	4.0	–	–	–	3.6	–	2.9 ¹	–	–	18.8
35	643-649	645.50-648.54	64.5	44.5	72.2	–	4.6	–	–	–	3.3	–	–	–	–	20.0
37	662-674	667.14-667.19	69.1	51.7	32.9	2.0	10.9	–	9.9	–	34.1	–	10.1 ¹	–	–	–
38	674-686	676.30-679.76	56.9	32.6	68.3	–	12.4	1.4	10.2	–	7.8	–	–	–	–	–
		677.51-677.51	65.1	45.5	82.5	1.3	4.7	–	–	–	6.9	–	4.6 ¹	–	–	–
		679.76-679.76	60.6	38.4	85.1	–	4.5	–	–	1.7	8.7	–	–	–	–	–
39	686-699	688.27-688.27	53.9	27.9	98.6	–	1.4	–	–	–	–	–	–	–	–	–
		690.89-690.89	58.1	34.6	80.7	1.8	3.3	–	–	–	9.1	–	–	5.2	–	–

¹ See text.